Anisotropic Magnetoresistance in Ferromagnetic 3d Alloys

T. R. McGUIRE AND R. I. POTTER

Abstract—The anisotropic magnetoresistance effect in $3d$ transition metals and alloys is reviewed. This effect, found in ferromagnets, depends on the orientation of the magnetization with respect to the electric current direction in the material. At room temperature, the anisotropic resistance in alloys of Ni-Fe and Ni-Co can be greater than 5%. The theoretical basis takes into account spin orbit coupling and d band splitting. Other properties such as permeability, magnetostriction, and Hall voltage have no simple relationship to magnetoresistance. Anisotropic magnetoresistance has an important use as a magnetic field detector for digital recording and magnetic bubbles. Such detectors because of their small size are fabricated using thin film technology. Film studies show that thickness, grain size, and deposition parameters play a significant role in determining the percentage change in magnetoresistance. In general, the change is smaller in films than bulk materials. Several tables and graphs that list bulk and film data are presented.

I. INTRODUCTION

A. Brief Description of the Anisotropic Magnetoresistance Effect

The discovery of anisotropic magnetoresistance in ferromagnetic metals was made by William Thomson [1] in Glascow in 1857. Thomson, honored as Lord Kelvin, was noted for his engineering contributions in addition to his scientific achievements. However, it was not until a century after his discovery of anisotropic magnetoresistance that it was put to a successful engineering use as a detection element in magnetic recording. It is the objective of this paper to review the fundamental work on magnetoresistance and indicate why it is a useful effect. Actual devices and their design problems are reviewed by Thompson, Romankiw, and Mayadas [2] in the paper following this one.

The subject of galvanomagnetism is a vast one, and our discussion will be restricted to one small part. There are three types of electrical resistance changes in ferromagnetic metals to be considered—those associated with changes in magnetization at a fixed temperature, those associated with changes of magnetization as caused by temperature changes, and those associated with the direction of magnetization relative to the current (also temperature dependent). It is the last effect, called by Smit [3] the orientation effect but called in this paper the anisotropic effect or ferromagnetic resistivity anisotropic, which will be discussed primarily in this paper.

Manuscript received February 10, 1975.

T. R. McGuire is with the IBM Research Laboratories, Yorktown Heights, N.Y. 10598.

R. I. Potter is with the IBM Research Laboratories, San Jose, Calif. 95193.

To define clearly the anisotropic magnetoresistance effect, consider the diagrams shown in Fig. 1. In Fig. 1a we show the spontaneous magnetization of a metal alloy such as $Ni_{0.9942}$ · $Co_{0.0058}$ from absolute zero to the Curie temperature. At room temperature we examine the anisotropic magnetoresistance for a cylindrical specimen, for which the demagnetizing tensor is known. The result is illustrated in Fig. 1b, where the upper curve is the condition for the magnetic moment M parallel to the electric current i and the bottom curve is the perpendicular orientation. Starting from an arbitrary resistivity characterized by a multidomain configuration, a small *internal* field of 50 Oe or less aligns domains giving $\rho_\parallel$ or $\rho_\perp$. For permalloy a few Oe is sufficient. This initial difference $\Delta\rho = \rho_\parallel - \rho_\perp$ is the anisotropic magnetoresistivity. The normalized quantity $\Delta\rho/\rho_{av}$, where $\rho_{av} \equiv \frac{1}{3}\rho_\parallel + \frac{2}{3}\rho_\perp$ (see Section II), is called the anisotropic magnetoresistivity ratio. It is a useful quantity for both basic understanding and engineering purposes, and can be obtained directly from $\Delta R/R$ without one needing to know the dimensions of the specimen.

If the internal magnetic field is now increased by several thousand Oe, the resistivities $\rho_\parallel$ and $\rho_\perp$ decrease uniformly and by the same amount as shown in Fig. 1b. This decrease in ρ is attributed to the increase in M above the spontaneous moment M_s caused by an applied field H, as marked by points a and b in Fig. 1a. It is an isotropic effect and has been discussed by Mott [4] in connection with the temperature dependence of resistivity of ferromagnetic metals and has to do with the scattering of conduction electrons into exchange split d bands. We note that at $77°K$ (Fig. 1c) the field dependence of both $\rho_\parallel$ and $\rho_\perp$ is changing in character. Finally at $4.2°K$ (Fig. 1d) there is an increase in resistivity with field due to the ordinary magnetoresistance effect briefly considered in the next section (IB). Field dependent effects can be large both at low temperatures and near the Curie temperature T_c, but we will not be concerned with them in any detail in this paper.

Anisotropic magnetoresistance as a phenomenological concept is simple to understand, and its measurement with modern instrumentation is fast and precise. The microscopic origin of the effect is, we believe, understood, but better than order-of-magnitude calculations are not so simple. For example, the fact that $\rho_\parallel$ is nearly always greater than $\rho_\perp$ at room temperature is not easily explained. Anisotropic magnetoresistance theory fits appropriately the remark of Meaden [5], "The theory of metallic resistance abounds in mysteries."

Although the anisotropic magnetoresistance effect has been investigated over a long time span, the work prior to 1945 is sometimes difficult to interpret because in some studies longitudinal resistivity ($\rho_\parallel$) was favored to the exclusion of transverse measurements ($\rho_\perp$). In many cases, the initial condition of the magnetic state of the specimen is not known and the measurement of $\rho_\parallel$ will not give a valid indication of $\Delta\rho$.
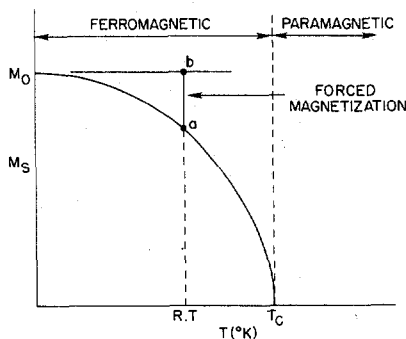
Fig. 1a. Variation of saturation magnetization M_S with temperature. The line ab marks the region of forced magnetization at room temperature. It is this additional magnetization as a function of applied field that causes the corresponding decrease in the magnetoresistance, as indicated in Fig. 1b.
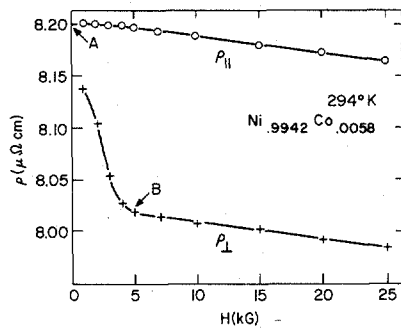

Fig. 1b. Resistivity of $Ni_{0.9942}Co_{0.0058}$ as a function of applied magnetic field at room temperature. The points A and B mark the selection of $\rho_\parallel$ and $\rho_\perp$ to determine the anisotropic magnetoresistivity associated with the orientation of the spontaneous moment M_S. The point B is at a higher applied field than A because of demagnetization.
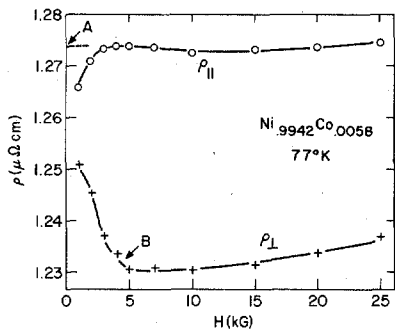

Fig. 1c. Resistivity of $Ni_{0.9942}Co_{0.0058}$ at 77°K. Because M_S has nearly reached the value of M_0 the normal increase in the ordinary magnetoresistivity with applied field is now observed. The points A and B mark values of $\rho_\parallel$ and $\rho_\perp$ associated with the anisotropic effect.
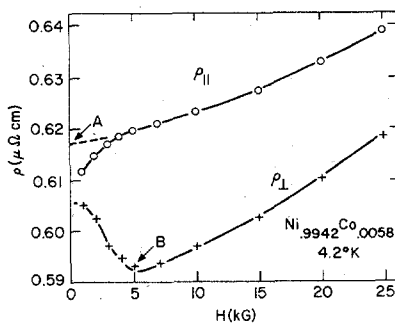

Fig. 1d. Resistivity of $Ni_{0.9942}Co_{0.0058}$ at 4.2°K (McGuire [20]).

The paper by McKeehan [6] is partly a review and lists over 40 references covering the period 1857 to 1930. McKeehan's objective was to study the longitudinal resistivity of nickel and permalloy as affected by both stress and magnetization. He showed that the longitudinal resistivity is approximately a function of the magnetic moment orientation alone and does not depend on whether a given orientation is produced by the application of a field or by elastic stress. Bozorth [7] further clarifies the magnetoresistance in terms of the domain theory and he was apparently the first one to show measurements of $\Delta\rho/\rho_{av}$ from both $\rho_\parallel$ and $\rho_\perp$ for the Ni-Fe alloy system, thus avoiding erratic results that may be caused by the initial state of the specimen. The Ni-Fe alloy results are given in Fig. 2. In addition, Bozorth showed that the effect of stress is more complicated than first reported. It depends on the particular alloy, its magnetostrictive coefficients, and the crystalline grain structure. Only in favorable cases will stress through magnetostriction align domains in the same way that a magnetic field would.

In Fig. 2 is illustrated another interesting problem associated with anisotropic magnetoresistance. What is the cause of the peak value of 5% for $\Delta\rho/\rho_{av}$ at the composition $Ni_{0.9}Fe_{0.1}$? There is also a corresponding behavior in the Ni-Co alloy system where a maximum in $\Delta\rho/\rho_{av}$ is found at the composition $Ni_{0.8}Co_{0.2}$. This effect was first observed by Shirakawa [8], [9], but the measurements of Van Elst [10] shown in Fig. 3 are more definitive.

Snoek [11] called attention to the maxima in anisotropic magnetoresistance and pointed out that they correlate with a magnetization corresponding to approximately one Bohr magneton per atom in the alloy. Zero magnetostriction was also attributed to those compositions at which $\Delta\rho/\rho_{av}$ is maximum. Snoek's observations stimulated new work on anisotropic magnetoresistance. Smit [3] and van Elst [10] both carried out comprehensive investigations touching on the points raised by Snoek and adding other correlations, such as zero extraordinary Hall voltage for alloys having a maximum in $\Delta\rho/\rho_{av}$. The possibility that the density of states curve may be of importance and the part played by spin-oribt interactions is also discussed.

The work of Smit, followed by that of van Elst, marked the beginning of a period of many new experimental and theoretical studies related to anisotropic magnetoresistance.
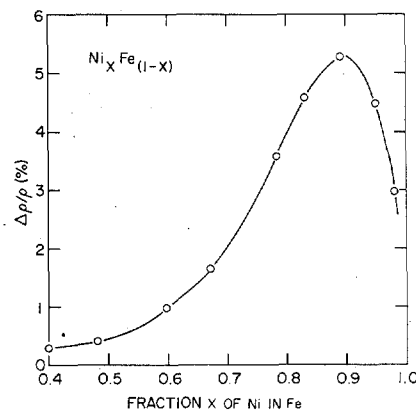

Fig. 2. Anisotropic magnetoresistivity ratio in percent for $Ni_xFe_{(1-x)}$ alloys at room temperature (Bozorth [7]).
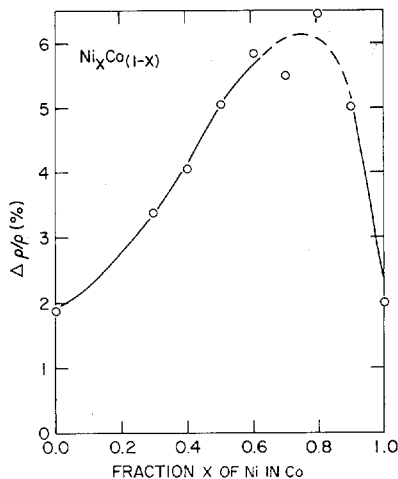
Fig. 3. Anisotropic magnetoresistivity ratio in percent for $Ni_xCo_{(1-x)}$ alloys (Smit [3] and van Elst [10]).

Many investigations of thin films were reported. Films, moreover, are important in device considerations.

B. Ordinary Galvanomagnetic Effects

Comparing the ordinary magnetoresistance of nonmagnetic metals with that of ferromagnets aids in our understanding of galvanomagnetic properties. All nonmagnetic metals exhibit an increase in electrical resistance as a function of applied field. In general the increase is proportional to B^2, but this can be more complicated both at high magnetic fields and low temperatures. In addition, the transverse magnetoresistance is larger than the longitudinal one. This relationship is directly opposite to that found in almost all cases for the ferromagnetic anisotropic effect. For the ordinary magnetoresistance [12] the anisotropy arises from the convoluted nature of the Fermi surface. In the case of thin films the resistivity is raised by a size effect phenomenon whereby the transverse geometry produces an increased amount of surface scattering. Surface scattering effects will be discussed in Section ID(2).

The ordinary magnetoresistance for several elements is illustrated in Fig. 4 in what is known as a reduced Kohler plot [13]. Such a plot follows the relation $\Delta\rho/\rho_0$ = function $(B\rho_\theta/\rho_0)$ where $\Delta\rho$ is the change in resistivity caused by a field B, and ρ_0 and ρ_θ are, respectively, the resistance in zero
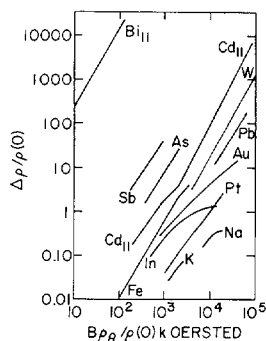

Fig. 4. A reduced Kohler plot for several metals, where ρ (0) is the resistivity in zero magnetic field, ρ_θ is the resistivity at the Debye temperature θ, and B is the magnetic field in kOe. (Jan [15]).

B and the resistance at the Debye temperature. ρ_θ normalizes the data for phonon scattering. From the log–log plot of Fig. 4, a B^2 fit is reasonable in most cases. As shown in Fig. 4, Fe behaves similarly to other nonferromagnetic multivalent elements. The Fe plot is from high field low temperature data [3] similar to that shown in Fig. 1d. Kohler's rule is discussed in Section IIB.

The ordinary magnetoresistivity has had a considerable amount of theoretical treatment. No magnetoresistive effects are predicted using only free electron theory [14]. To obtain ordinary magnetoresistance, we must go to more complicated Fermi surfaces than the single spherical surface of the free electron model. When this is done, the velocity of each conduction electron depends not only on the applied electric field but also on the electron's position on the Fermi surface. It is possible to account for magnetoresistivity effects in the case of some metals and semiconductors when both electron and hole conduction are present in two separate spherical bands. In this way, the quadratic dependence shown in Fig. 4 is explained. However, this model gives a nonzero magnetoresistance only for the transverse geometry. The review article by Jan [15] covers a detailed discussion of ordinary magnetoresistance effects. Symmetry arguments [16] can be used to show that, in nonmagnetic materials, magnetoresistance must be an even function of the field and the Hall effect an odd function of the field.

C. Extraordinary or Anisotropic Magnetoresistance Effect

As defined earlier, the extraordinary magnetoresistivity or ferromagnetic resistivity anisotropy depends on the direction of the spontaneous magnetization, whereas the ordinary effect depends only on the direction and magnitude of the applied field. The electric field due to the extraordinary effect is given in vector form by

$$E = \rho_\perp j + \alpha(j \cdot \alpha)(\rho_\| - \rho_\perp) + \rho_H \alpha \times j \qquad (1)$$

where j is the current density and α is a unit vector in the direction of the magnetic moment of the single domain sample. $\rho_\|$ and $\rho_\perp$ are, respectively, the resistivities parallel and perpendicular to α. The last term in equation (1) gives the extraordinary Hall electric field. For a truly randomly-demagnetized specimen the resistivity in zero field, ρ_0', is approximately (see Section IIA) $\rho_{av} \equiv \frac{1}{3}\rho_\| + \frac{2}{3}\rho_\perp$. If the magnetoresistance is defined as the relative change in resistivity between a fully magnetized sample and one which is in the demagnetized state, we have

$$\frac{\Delta\rho_\perp}{\rho_{av}} = \frac{\rho_\perp - \rho_{av}}{\rho_{av}} \quad \text{and} \quad \frac{\Delta\rho_\|}{\rho_{av}} = \frac{\rho_\| - \rho_{av}}{\rho_{av}}.$$

In principle, knowing ρ_{av} and either $\rho_\|$ or $\rho_\perp$ is sufficient, but experimentally, it is the zero field resistivity ρ_0 and not ρ_{av} that is measured. It is better, therefore, to measure both $\rho_\perp$ and $\rho_\|$ and define

$$\frac{\Delta\rho}{\rho_{av}} = \frac{\rho_\| - \rho_\perp}{\frac{1}{3}\rho_\| + \frac{2}{3}\rho_\perp}.$$

TABLE I
Elements

Alloy	Temp °K	$\Delta\rho/\rho_0$ %	ρ_0 μΩcm	$\Delta\rho$ μΩcm	$4\pi M^*$ G	n_B^*	T_C^* (X°)	Ref	Comment
Fe	300	0.2	9.8	.02	21580		1043	[17]	
	77	0.3	.64	.002	21800	2.2		[18]	
Co	300	1.9	13.0	.25	17900	1.7	1388	[19]	
Ni	300	2.02	7.8	.16	6084		631	[20]	
	77	3.25	.69	.023	6350	.60			
Gd	300	0	130	0			293	[21]	
	200	0.2	95	.19	14500			[22]	
	77	6.0	27	.16	18700	7.5			
Ho	24	22	11	2.43			19	[22]	
	4.2	32	7	2.24	23200	8.5		[23]	polycrystalline
Nd	1.38	±5.0	2.21	±.1				[24]	a

*The values of $4\pi M$, n_B, and T_c are taken from sources [9], [98], [99], in addition to the original reference. In some cases the values for alloys represent estimates based on closely related compositions.

[a]Neodymium is antiferromagnetic in zero field but developes a ferromagnetic component above 12 kOe. This behavior is evidently responsible for the change in sign of $\Delta\rho$ from minus values at low field to positive values as H is increased.

The difference between ρ_0 and ρ_{av} is relatively unimportant in this ratio, and we shall use them interchangeably. In a circular, single domain, film sample where M makes an angle ξ with j we find directly from equation (1) that

$$\rho(\xi) = \rho_\perp \sin^2 \xi + \rho_\| \cos^2 \xi$$

or

$$\rho(\xi) = \rho_\perp + \Delta\rho \cos^2 \xi. \qquad (2)$$

Table I gives values of $\Delta\rho$, ρ_0, $\Delta\rho/\rho_0$, and M for several elements at room temperature. This table and Figs. 2 and 3 illustrate quantitatively the following important features:

(a) Neither $\Delta\rho$ or ρ_0 is dependent on M in a simple way.

(b) $\rho_\|$ is generally, but not always, greater than $\rho_\perp$.

(c) Alloy systems such as Ni-Fe and Ni-Co also vary in a manner unrelated to M or ρ_0 (see Figs. 2 and 3).

Where does ordinary theory fail in explaining the preceding facts? First, if we consider M as representing an internal field $B = 4\pi M$, then increasing M should increase the magnetoresistance effect, but this does not happen. Second, in the ordinary case $\rho_\perp > \rho_\|$ where just the opposite behavior is the rule here. It is obvious that the theory of the ferromagnetic resistivity anisotropy must rest on a different analysis than that used for the ordinary effects.

D. Related Properties

Several physical properties of magnetoresistive materials are important to a basic understanding of the anisotropic effect and its usefulness in devices.

(1) Resistivity: The resistivity of any ferromagnetic metal (ρ_{av}) is a basic parameter affecting the anisotropic magnetoresistance ratio ($\Delta\rho/\rho_{av}$). Although output signals in a magnetoresistive device are proportional to $\Delta\rho$, the ratio $\Delta\rho/\rho_{av}$ is a reasonable figure of merit for device applications because power dissipation is proportional to ρ_{av}. From simple trans-

port theory the electrical conductivity is given as $\sigma = Ne\mu$ where N is the number of electrons per unit volume and μ is the mobility, which is the velocity the charge carriers reach in unit electric field strength. Using kinetic theory, the electrical resistivity can be shown to be $\rho = 1/\sigma = mv_F/Ne^2 l_0$. Here v_F the velocity of conduction carriers (of charge e and mass m) at the Fermi surface, and l_0 is the average mean free path, which is equal to τv_F where τ is the average time between collisions. To calculate ρ one must know the value of l_0 or τ.

The charge carriers can be scattered by phonons, which will give rise to a temperature-dependent resistivity ρ_T, and also by material parameters characterized as a static contribution ρ_s. The static effects are caused by conduction electron scattering from imperfections and impurity atoms. In thin films, grain boundaries [25], surface scattering [26], stacking faults [27], and stress [28] can be important sources of resistivity. As we shall subsequently discuss, various sources of resistivity can raise $\rho = \rho_T + \rho_s$ without a corresponding increase in the magnetoresistance anisotropy $\Delta\rho$. In most cases, binary alloys are used for magnetoresistance devices. Each constituent of a binary alloy can be regarded as an impurity with respect to neighboring ions of the other constituent. Impurities act as scattering centers for several reasons:

(a) The charge of the impurity atom differs from that of the host lattice.

(b) The crystal lattice becomes distorted because of the size of the impurity atom.

(c) The conduction electron density (N) is changed.

(d) The Fermi surface is altered.

In the case of items (a) and (b), the periodicity of the lattice is affected and the potential U_A in the neighborhood of the impurity atom A will differ from that in the neighborhood of host atoms B. Under these conditions, the average resistivity can be shown [29] to be

$$\rho_0 = C \times (1 - x),$$

where C is a constant.

Fig. 5 shows the resistivity at room temperature for the alloy systems Ni-Cu, Ni-Co, and Ni-Fe. For Ni-Cu a parabolic dependence on composition is often referred to as Nordheim's
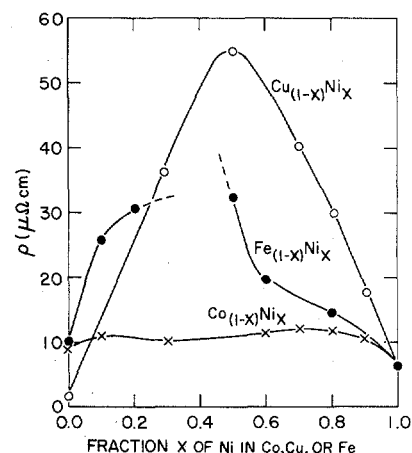

Fig. 5. Resistivity of the binary alloy systems $Ni_xFe_{(1-x)}$, $Ni_xCo_{(1-x)}$, and $Ni_xCu_{(1-x)}$ (Bozorth [9]).

rule. Ni-Cu has a much higher resistivity than either Ni-Co or Ni-Fe because Ni and Cu do not form a common d band. In Ni-Co a common d band is known to exist [30]. The band structure of transition metal alloys can thus represent an additional complication. This makes it difficult to apply simple rules such as Nordheim's to predict the behavior of a new alloy system. The conclusion concerning resistivity is that certain $3d$ impurity atoms, for example Cu, Cr, and Mn [31], increase the resistance of pure Ni to a much greater extent than other elements such as Co or Fe. Unless some significant advantage occurs regarding properties such as corrosion, magnetostriction, or thermal stability, Cu, Cr, or Mn are not a good choice for alloys for magnetoresistance applications.

(2) Thin Film Resistivity: It is well known that film resistivity increases as films become thinner. This phenomenon, in which surface scattering of the conduction electrons becomes important, is called the size effect. The resistivity noticeably increases when the mean free path (l) of the conduction electrons is comparable to the film thickness (t). Perhaps the simplest way to view this effect is that the surface is an additional obstical to the electrons motion. This shortens the mean free path and thereby lowers the conductivity in a systematic way. In order for this to occur, electrons must be diffusely scattered at the surface, a condition supported by many observations [26]. Under conditions of diffuse scattering the following approximations have been given by Fuchs [32] and Sondheimer [33]. For a thick film where $l_0 < t$,

$$\rho = \rho_0 [1 + \tfrac{3}{8}(l_0/t)] \tag{3}$$

and for very thin films, where $t \ll l_0$,

$$\rho = \rho_0 \frac{4l_0}{3} \frac{1}{[\ln(l_0/t) + 0.423]}$$

where ρ_0 is the bulk resistivity and ρ is the measured value. Equation (3), the thick film approximation, is a reasonable fit over a wide range of l_0/t values even when the condition $l_0 < t$ is no longer satisfied. A detailed discussion as well as a graphical comparison of the approximate expressions with the complete solution is given by Hall [34]. Shown in Fig. 6 are resistivity data for $Ni_{0.82}Fe_{0.18}$ films as measured by Mitchell *et al.* [35]. The fit to equation (3) gives a bulk value of $\rho_0 = 18 \times 10^{-6}$ Ωcm and $l_0 = 300$ Å. Both values are reasonable although somewhat high. However, it is important that films with thickness over 500 Å have almost the bulk value for ρ. Fig. 6 also shows films prepared by Williams and Mitchell using a high rate of evaporation of 1000 Å/s. These films have higher resistivities.

In the measurements of the resistivity of $Ni_{0.82}Fe_{0.18}$ films shown in Fig. 6 the effect of grain boundaries has been neglected. Grain boundaries mark the interface of two crystals that have different orientations and thus interupt the regularity of the lattice. A recent study (Fig. 7) [36] of $Ni_{0.7}Co_{0.3}$ takes into account grain boundary scattering. This is done by annealing the films at 400°C for one hour in a vacuum, which cause the grain size to grow. The microstructure of the films before and after heat treatment is obtained from transmission
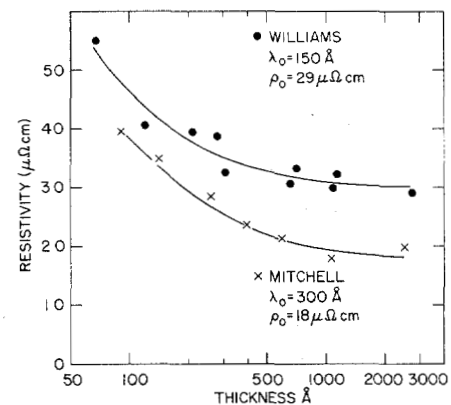
Fig. 6. Comparison of the resistivity as a function of thickness of two series of $Ni_{0.82}Fe_{0.18}$ films. The films were prepared using different evaporation rates; the lower resistivity films (x—Mitchell *et al.* [35]) at 170 A/s and the higher resistivity films (•—Williams and Mitchell [35]) 1000 Å/s.

electron microscopy where high resolution pictures with a magnification of 10^5 clearly show the grain structure and size and demonstrate that the annealed samples have very large grains. This lowers the resistivity.

Mayadas and Shatzkes [37] use a grain boundary model consisting of a series of partially reflecting ($\Re$) planes, randomly spaced but with normals in the film plane. An approximate expression is given for obtaining the grain boundary resistivity ρ_g:

$$\rho_g l_g = \frac{3}{2} \rho_0 l_0 \left(\frac{\Re}{1 - \Re} \right). \tag{4}$$

where l_g is a fictitious mean free path associated with grain boundaries. ρ_0 and l_0 are for bulk materials (where grain boundary effects are negligible), and $\Re$ is a reflection coefficient representing the probability of the conduction electron's path being terminated by the grain boundary. In Fig. 7 are given the resistance data for the $Ni_{0.7}Co_{0.3}$ films as a function of thickness for the annealed and as deposited films. Using equations (3) and (4) it is possible to estimate that the grain boundaries have a reflection coefficient $\Re$ of about 0.17. The annealed specimens give $\rho_0 \approx 1.45 \times 10^{-6}$ Ωcm and $l_0 \approx 150$ Å as the bulk values.
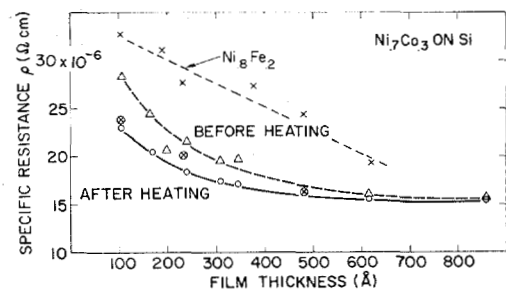
Fig. 7. Resistivity as a function of thickness for $Ni_{0.7}Co_{0.3}$ films shown as deposited (△—before heating) and after annealing one hour at 400°C in vacuum (○—after heating). For comparison, several data points for $Ni_{0.8}Fe_{0.2}$ are shown (X—before heating and ⊗—after heating) (McGuire *et al.* [36]).

The technology and science of thin films represents an enormous area of research [26] [34]. Deposition parameters, substrates, film roughness, and strain conditions all must be taken into consideration in interpreting results. Film thickness and grain boundaries adequately explain gross changes. In the last section of this paper (III B) consideration will be given to the preceding conditions with reference to the magnetoresistivity anisotropy.

(3) Permeability: As illustrated in Figs. 2 and 3, there is observed a maximum of the anisotropic magnetoresistance ratio in the Ni-Fe and Ni-Co alloy systems. The question arises as to the correlation of other magnetic properties with these maxima. Because of its commercial importance, the Ni-Fe system has been widely studied. In the permalloy region, large values of initial permeability, μ_0 and maximum permeability are found. At approximately the composition $Ni_{0.78}Fe_{0.22}$ a sharp maximum in μ_0 is produced by heat treatment [9] as shown in Fig. 8. At this composition, the crystalline anisotropy K_1 and the magnetostriction λ both become very small. The high permeability is in part a consequence of K and λ passing through zero. In addition it is necessary that the materials exhibit few imperfections since the initial permeability is determined by reversible domain wall motion.

In the Ni-Co alloy system, the permeability is reasonably high in the composition region ($Ni_{0.8}Co_{0.2}$) where $\Delta\rho/\rho_0$ is large, as indicated in Figs. 3 and 9. This system is similar to the Ni-Fe one in that the composition corresponding to zero K roughly matches the composition for maximum $\Delta\rho/\rho_0$. It is dissimilar in that zero λ and maximum $\Delta\rho/\rho_0$ occur at considerably different compositions.

Two considerations are apparent. First, in both Ni-Fe and Ni-Co it is fortunate and useful to have this correspondence between μ_0 and $\Delta\rho/\rho_0$ because of the practical application of magnetoresistance for high sensitivity magnetic field sensors. Second, it is an interesting scientific question concerning the fundamental reasons for the existence of such a correlation. Initial permeability in itself cannot be regarded as a funda-
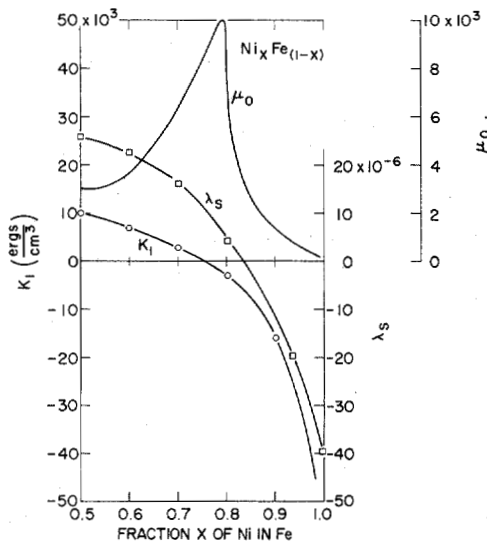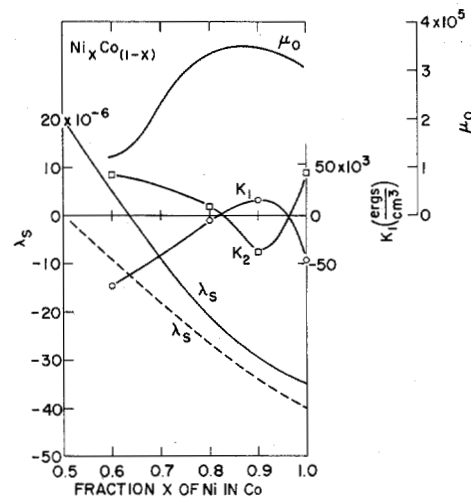

Fig. 9. Crystalline anisotropy K_1 and K_2, saturation magnetostriction λ_s, and initial permeability μ_0 for $Ni_xCo_{(1-x)}$ (Bozorth [9], Went [39], Yamamoto and Nakamichi [40]).

mental parameter because it is structure sensitive and depends on such procedures as heat treatment. Unfortunately, there appears to be no systematic study of how the anisotropic magnetoresistivity and μ_0 are related in $Ni_{0.78}Fe_{0.22}$ permalloy. Of some interest in this connection is moly-permalloy. The composition $Ni_{0.79}Fe_{0.15}Mo_{.05}$ has one of the highest initial permeabilities. The exact reason for this enhancement of μ_0 is not known, but it may be related to both λ and K being simultaneously zero. However, molybdenum raises the resistivity of the alloy which is detrimental to the ratio $\Delta\rho/\rho_0$, which at room temperature is only about 0.5% [38].

(4) Magnetostriction: Snoek [11] originally suggested that alloys with zero magnetostriction had maximum magneto-resistance. Is such a relationship found experimentally and if so why? There is also the practical consideration regarding the elimination of magnetostrictive noise when such alloys are used. Thus the zero λ depicted in Figs. 8 and 9 for Ni-Fe and Ni-Co alloys has a twofold interest.

Plotted in Figs. 8 and 9 is the saturation value of spontaneous magnetostriction λ_s. In actual measurements, the induced strain which gives λ_s comes from the change in dimensions of the material upon going from the demagnetized state to the magnetized state where all the magnetic domains are aligned. Once alignment occurs, further application of an applied magnetic field will increase the saturation magnetization. Associated with this is an increase in λ called forced magnetostriction. We shall not be concerned with the forced component of λ but only the spontaneous one λ_s, which is most closely identified with the conditions under which the magnetoresistance anisotropy is determined.

Since a field will change the dimensions of a ferromagnetic material due to domain rotation, there is a corresponding rotation of domains when the sample is strained [6], [7]. Because of the anisotropic magnetoresistance effect, strain effects can be detected by resistivity measurements. When λ_s is positive (e.g., $Ni_{0.5}Fe_{0.5}$) there is a rotation of the domain magnetization toward the strain axis; when λ_s is negative ($Ni_{0.9}Fe_{0.1}$)

Fig. 8. Crystalline anisotropy K_1, saturation magnetostriction λ_s and initial permeability μ_0 for $Ni_xFe_{(1-x)}$ (Bozorth [9]).

the magnetization rotates perpendicular to the strain axis. We do not view the relationship between λ_s and $\Delta\rho/\rho_0$ under these conditions to have fundamental significance. However, the concept is useful in device design and in understanding the origin of noise problems.

Is the zero λ_s, shown in Figs. 8 and 9 for Ni-Fe and Ni-Co, related to the maximum in $\Delta\rho/\rho_0$? For the Ni-Co system some confusion exists concerning λ_s. However, measurements by Went [39], upon which Snoek drew his conclusions, agree with a later study by Yamamoto and Nakamichi [40]. For Ni_xCo_{1-x}, λ_s is zero at $x \approx 0.65$. This does not correspond to a maximum in $\Delta\rho/\rho_0$, which occurs at $x \approx 0.80$. Even Ni-Fe does not have a good match with $\lambda_s \approx 0$ at $x = 0.83$, because $\Delta\rho/\rho_0$ has its largest value at $x \approx 0.10$. Of interest in this context is the Cu-Ni-Fe system studied by Ashworth et al. [41] and shown in Fig. 10. These alloys remain fcc, but there is no obvious correspondence between λ_s and $\Delta\rho/\rho_0$ for 20°K data.

Although we conclude that experimentally there is little justification for relating λ_s to $\Delta\rho/\rho_0$, theoretical discussion shows that the two are not totally unrelated. This is because spin-orbit interactions are invoked in both phenomena [41], [42] and also electron band filling may be of importance [10], [39]. Thus a more complex relationship might exist in which both are dependent on a third, common, set of conditions.

(5) Spontaneous Hall Effect: The Hall effect is a property related to magnetoresistance but of more significance to theoretical understanding in metals than to engineering use. Similar to both λ and $\Delta\rho/\rho_{av}$, the Hall effect in ferromagnetics can be divided into two parts: the ordinary part, which is proportional to B, and the extraordinary or spontaneous part, dependent upon M. The Hall resistivity per unit current density is often written as

$$\rho_H = R_0 B + R_s M,$$

where R_0 is generally a smaller quantity than R_s. The ordinary coefficient, R_0, presents no special problems in inter-
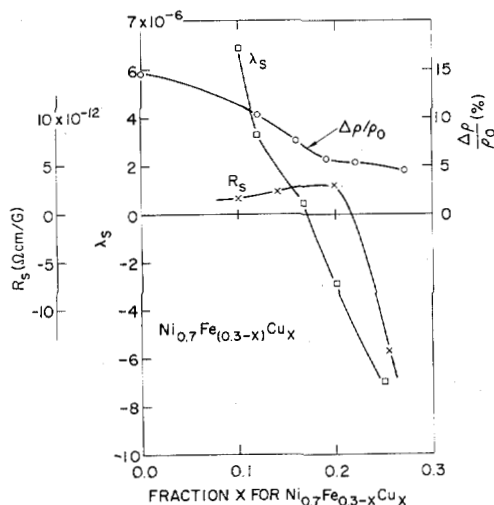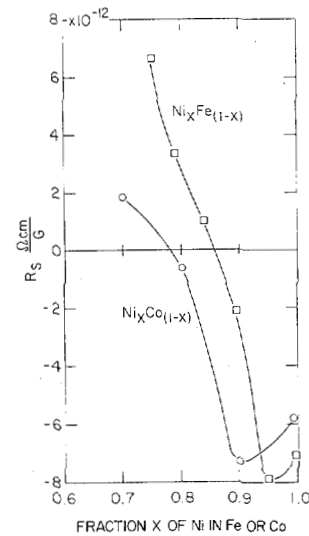

Fig. 11. Spontaneous Hall coefficient at room temperature for $Ni_xFe_{(1-x)}$ (□) and $Ni_xCo_{(1-x)}$ (○) as a function of composition, x (Smit [43]).

pretation over those associated with other nonferromagnetic multivalent metals. The approach involves consideration of the Fermi surfaces [15] of the respective metals.

The interpretation of R_s, however, has long been a problem because, in terms of only the Lorentz force on the conduction electrons, magnetic fields equivalent to several times the value of $4\pi M$ (the internal B field) are necessary to explain the magnitude of R_s in many cases. A dominant mechanism in many theoretical papers [3], [43] to [47] is the spin-orbit interaction with various degrees of complexity.

Of singular interest in connection with magnetoresistance is that in at least three alloy systems R_s changes sign (with composition) even though R_0 remains of the same sign. In Ni-Fe and Ni-Co, R_s is zero close to the composition where $\Delta\rho/\rho_{av}$ is maximum, as is shown in Fig. 11. The ternary system NiFeCu (Fig. 10) also exhibits an R_s which goes through zero but it does not appear that $\Delta\rho/\rho_{av}$ has a maximum value for this concentration. However, Ashworth et al. [41] describe the behavior of $\Delta\rho/\rho_0$ with respect to $R_s = 0$ as having a ridge-like appearance when viewed on the ternary diagram.

Both Smit [43] and Berger [47] have discussed the zero value of R_s. Smit concludes that the Hall effect must be caused by skew scattering due to the role that the spin-orbit interactions plays when the conduction electrons are scattered by impurities or phonons. In the case of the purest sample of Ni, R_s goes to zero as the temperature approaches zero °K. A general behavior is that $R_s \approx \rho(T)^m$ where m can have a value of 1.4 to 2. The question of why R_s is zero at certain compositions of NiCo and NiFe is not directly considered.

Berger originally based his discussion on the appearance of an orbital degeneracy at the Fermi level at compositions when R_s became zero. Thus asymmetric scattering due to a spin-orbit interaction would become symmetrical. In subsequent papers, Berger [48], [49] introduces a nonclassical "side-jump" mechanism as an explanation for the Hall effect. The "side-jump" effect is assumed by him to be especially important at room temperature and at higher temperatures.

The problem also has been considered by Luttinger [50],

Fig. 10. Anisotropic magnetoresistivity ratio, saturation magnetostriction λ_s, and spontaneous Hall coefficient R_s for $Ni_{0.7}Fe_{(3-x)}Cu_x$ at 20°K (Ashworth et al. [41]).

making use of the transport theory of Kohn and Luttinger [51] that includes off-diagonal parts of the density matrix.

E. Thin Film Work

Thin film deposition is the primary method of fabricating magnetoresistance devices, and this fact underscores the importance of anisotropic magnetoresistance in films. The advantages of thin film technology include the ability to batch-fabricate and to construct magnetic recording head arrays for multi track use. It offers complete processing on a single chip. From an electrical and magnetic viewpoint, the small volume of the film in such devices leads to high data density, a good electrical impedance match, and allows the gaps between the various films comprising the head to be reduced. The detection of magnetic bubbles also uses thin film magnetoresistors.

Any survey of film data indicates immediately that the majority of papers report only on permalloy films. This is a consequence of their engineering importance. The remaining films that have been studied are binary alloy $Ni_{0.70}Co_{0.30}$ and pure elements such as Ni and Co. We summarize here some of the principal results of a general nature on films:

(a) The anisotropic magnetoresistance ratio depends on thickness, grain size, and film surface conditions.

(b) There is a large preparation dependent variation in the magnetoresistance involving parameters such as vacuum quality, substrate temperatures, and deposition rates.

(c) In many papers, the resistivity ratio $\Delta\rho/\rho_0$ is given without any additional information concerning the specific resistance ρ_0 of the films.

(d) Film measurements are reliable only at room temperature. At low temperatures surface scattering dominates and interpretation of magnetoresistance data is difficult.

(e) Associated magnetic parameters such as coercivity, field induced anistropy and permeability are also difficult to control.

In Section III, we will attempt to illustrate and document the behavior of the anisotropic magnetoresistance in films and also in tabular form list both bulk and film alloys that have been so far reported. Section II is a description of anisotropic magnetoresistance in ferromagnets based on both symmetry and microscopic theory.

II. THEORY OF EXTRAORDINARY MAGNETORESISTANCE

A. Phenomenological Theory: Expression Arising from Symmetry

In this section, the basis for the well-known $\cos^2 \xi$ variation (Eq. 2) in the resistivity of polycrystalline samples is discussed, where ξ is the angle between the current density and magnetization. Relations are obtained between quantities for demagnetized or magnetically saturated single crystals and corresponding quantities for polycrystalline samples. The treatment parallels that given by Birss [52] for magnetostriction.

Let α_i be direction cosines of the magnetization with respect to the crystallographic axes of a single crystal sample. Experimentally, a known current density with components J_j relative to the crystallographic axes is established, and this produces electric field components

$$E_i = \rho_{ij}(\hat{\alpha}) J_j.$$

The resistivity tensor ρ_{ij} is a function of the unit vector $\hat{\alpha}$ and is expanded in a MacLaurin's series

$$\rho_{ij}(\hat{\alpha}) \ a_{ij} + a_{ijk}\alpha_k + a_{ijk}\alpha_k \alpha_l + \cdots$$

where the Einstein summation convention is understood. The resistivity tensor can be divided into a symmetric part

$$\rho_{ij}^s = \tfrac{1}{2} (\rho_{ij} + \rho_{ji})$$

and an antisymmetric part

$$\rho_{ij}^a = \tfrac{1}{2} (\rho_{ij} - \rho_{ji}).$$

Onsager's theorem [53] applied to a saturated crystal gives

$$\rho_{ij}(\hat{\alpha}) = \rho_{ji}(-\hat{\alpha})$$

so that ρ_{ij}^s is an even function of the α_i and ρ_{ij} is an odd function. The associated electric fields E^s and E^a are attributed to generalized magnetoresistance and Hall effects, respectively.

The tensors with elements a_{ij}, a_{ijk}, a_{ijkl}, etc. simplify due to crystal symmetry. If t_{ij} are the elements of a transformation matrix that leaves the crystal unchanged, then

$$a'_{mn \cdots z} = t_{mi}t_{nj} \cdots t_{zr}a_{ij \cdots r}$$

must be the same as $a_{ij \ldots r}$. For example, if the crystal is invariant under a 90° rotation about the z axis, described by

$$t = \begin{pmatrix} 0 & -1 & 0 \\ 1 & 0 & 0 \\ 0 & 0 & 1 \end{pmatrix},$$

then

$$a'_{12} = t_{1i}t_{2j}a_{ij} = -a_{21}$$

must be the same as a_{21}, which means $a_{21} = 0$. Listed in Table I, from Birss [54], are the nonzero elements for iron and nickel, which belong to point group $m3m$. The magnetoresistivity tensor ρ^s through fifth order in the α_i is

$$\rho^s = \begin{pmatrix} C'_0 + C'_1\alpha_1^2 + C'_2\alpha_1^4 + C'_3\alpha_2^2\alpha_3^2 & C'_4\alpha_1\alpha_2 + C'_5\alpha_1\alpha_2\alpha_3^2 & C'_4\alpha_1\alpha_3 + C'_5\alpha_1\alpha_3\alpha_2^2 \\ C'_4\alpha_1\alpha_2 + C'_5\alpha_1\alpha_2\alpha_3^2 & C'_0 + C'_1\alpha_2^2 + C'_2\alpha_2^4 + C'_3\alpha_3^2\alpha_1^2 & C'_4\alpha_2\alpha_3 + C'_5\alpha_2\alpha_3\alpha_1^2 \\ C'_4\alpha_1\alpha_3 + C'_5\alpha_1\alpha_3\alpha_2^2 & C'_4\alpha_2\alpha_3 + C'_5\alpha_2\alpha_3\alpha_1^2 & C'_0 + C'_1\alpha_3^2 + C'_2\alpha_3^4 + C'_3\alpha_1^2\alpha_2^2 \end{pmatrix}$$

where

$$C'_0 \equiv a_{11} + a_{1122} + a_{111122},$$

$$C'_1 \equiv a_{111} - a_{1122} - 2a_{111122} + a_{112211},$$

$$C'_2 \equiv a_{111111} + a_{111122} - a_{112211},$$

$$C'_3 \equiv a_{112233} - 2a_{111122},$$

$$C'_2 \equiv a_{2323} + a_{111212},$$

$$C'_5 \equiv a_{112323} - a_{111212}.$$

The resistivity along the current direction $\hat{\beta}$ is

$$\rho(\hat{\alpha}, \hat{\beta}) = \frac{J \cdot E}{|J|^2} = \frac{J_i \rho_{ij} J_j}{J_i J_i} = \beta_i \rho_{ij}^s \beta_i$$

since $\beta_i \rho_{ij}^a \beta_j = 0$. This is customarily written in the form

$$\rho(\hat{\alpha}, \hat{\beta}) = C_0 + C_1(\alpha_1^2 \beta_1^2 + \alpha_2^2 \beta_2^2 + \alpha_3^2 \beta_3^2)$$
$$C_2(\alpha_1 \alpha_2 \beta_1 \beta_2 + \alpha_2 \alpha_3 \beta_2 \beta_3 + \alpha_3 \alpha_1 \beta_3 \beta_1)$$
$$C_3(\alpha_1^2 \alpha_2^2 + \alpha_2^2 \alpha_3^2 + \alpha_3^2 \alpha_1^2)$$
$$C_4(\alpha_1^4 \beta_1^2 + \alpha_2^4 \beta_2^2 + \alpha_3^4 \beta_3^2)$$
$$C_5(\alpha_1 \alpha_2 \alpha_3^2 \beta_1 \beta_2 + \alpha_2 \alpha_3 \alpha_1^2 \beta_2 \beta_3 + \alpha_3 \alpha_1 \alpha_2^2 \beta_3 \beta_1),$$

which follows with the aid of the identity

$$\alpha_1^2 \alpha_2^2 \beta_3^2 + \alpha_2^2 \alpha_3^2 \beta_1^2 + \alpha_3^2 \alpha_1^2 \beta_2^2 = \alpha_1^4 \beta_1^2 + \alpha_2^4 \beta_2^2 + \alpha_3^4 \beta_3^2$$
$$- (\alpha_1^2 \beta_1^2 + \alpha_2^2 \beta_2^2 + \alpha_3^2 \beta_3^2) + \alpha_1^2 \alpha_2^2 + \alpha_2^2 \alpha_3^2 + \alpha_3^2 \alpha_1^2.$$

The constants C_i are $C_0 = C_0'$, $C_1 = C_1' - C_3'$, $C_2 = 2C_4'$, $C_3 = C_3'$, and $C_4 = C_2' + C_3'$.

$$C_5 = 2C_5' = 2a_{112323} - 2a_{111212}.$$

The preceding expression for $\rho(\hat{\alpha}, \hat{\beta})$ indicates, for example, that a cubic single-crystal sample magnetized along one of its crystallographic axes (the z axis, for example) exhibits a resistivity of the form

$$\rho = C_0 + C_i \cos^2 \theta + C_4 \cos^4 \theta + \cdots$$

where θ is the polar angle. In this example, θ also happens to be the angle between the magnetization and current-density vectors. A $\langle 110 \rangle$ directed magnetization results in

$$\rho = C_0 + \frac{1}{4} C_3 + \frac{1}{2} (C_1 + \frac{1}{2} C_4 + C_2 \sin \phi \cos \phi) \sin^2 \theta$$

where again θ and ϕ give the current direction with respect to the crystallographic axes.

Device applications invariably make use of polycrystalline films, making it of interest to consider an average of $\rho(\hat{\alpha}, \hat{\beta})$ over a large number of randomly oriented crystallites. The polycrystalline average can be performed by choosing $\hat{\alpha}$ to lie within a cone about an arbitrary current direction $\hat{\beta}$, with $\hat{\alpha} \cdot \hat{\beta} = \cos \xi$, and evaluating

$$\rho_{\text{poly}} = \frac{1}{8\pi^2} \int_0^{2\pi} d\psi \int_0^{\pi} d\theta \int_0^{2\pi} d\phi\, \rho(\hat{\alpha}, \hat{\beta}),$$

where ψ is an angle that locates $\hat{\alpha}$ within the cone as shown in Fig. 12. Birss [55] has carried out these integrations for the saturation magnetostriction $\lambda_s(\hat{\alpha}, \hat{\beta})$, which has the same
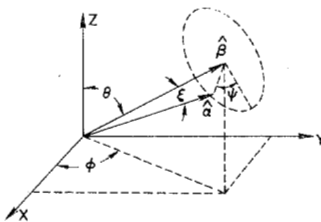

Fig. 12. Coordinate system for polycrystalline average.

form as $\rho(\hat{\alpha}, \hat{\beta})$. He obtains, in our notation,

$$\rho_{\text{poly}} = \rho_0 + \rho_1 \cos^2 \xi$$

where ξ is the angle between M and J and where

$$\rho_0 = C_0 + \frac{1}{5} C_1 - \frac{1}{10} C_2 + \frac{1}{5} C_3 + \frac{3}{35} C_4 - \frac{1}{70} C_5$$

and

$$\rho_1 = \frac{2}{5} C_1 + \frac{3}{10} C_2 + \frac{12}{35} C_4 + \frac{3}{70} C_5.$$

Note that only the cosine-squared term survives the average; it is not simply the second lowest order term in a series expansion.

Another quantity of interest is the resistivity of the demagnetized state. This depends on the sign of the first magnetocrystalline anisotropy constant, which determines the easy directions of magnetization. These are the $\langle 111 \rangle$ directions in materials such as nickel, with a negative constant, and the $\langle 100 \rangle$ directions in materials such as iron. The resistivity of a demagnetized, multidomain, *single crystal* is obtained by simply setting $\hat{\alpha}$ along any one of the $\langle 111 \rangle$ or $\langle 100 \rangle$ directions as appropriate. The argument depends on the magnetization within each domain pointing along an easy direction and not on the magnetization of all domains summing to zero. The resistivity of a demagnetized polycrystal is obtained by setting $\hat{\alpha}$ along an easy axis and averaging over $\hat{\beta}$. The result is

$$\rho_{\text{poly, demag}} = C_0 + \frac{1}{3} C_1 + \frac{1}{3} C_4$$

for $\langle 111 \rangle$ easy directions, and

$$\rho_{\text{poly, demag}} = C_0 + \frac{1}{3} C_1 + \frac{1}{3} C_3 + \frac{1}{9} C_4$$

for $\langle 100 \rangle$ easy directions. For single crystals with $\langle 111 \rangle$ easy directions, such as nickel, and with $\rho_\parallel$ and $\rho_\perp$ the resistivities when the magnetic moment is constrained along a hard direction (e.g., z axis),

$$\rho_{\text{poly, demag}} = \frac{1}{3} \rho_\parallel + \frac{2}{3} \rho_\perp$$

up through at least fifth order in the α_i; but in general the relation (for either single- or poly-crystals)

$$\rho_{\text{demag}} = \frac{1}{3} \rho_\parallel + \frac{2}{3} \rho_\perp \equiv \rho_{\text{av}}.$$

is only approximate.

The change in resistivity obtained upon magnetizing an initially demagnetized polycrystalline sample with current either parallel or perpendicular to the magnetization is

$$\rho_\parallel - \rho_{\text{demag}} = \frac{4}{15} C_1 + \frac{1}{5} C_2 + \frac{1}{5} C_3 + \frac{2}{21} C_4 + \frac{1}{35} C_5$$
$$\rho_\perp - \rho_{\text{demag}} = -\frac{2}{15} C_1 - \frac{1}{10} C_2 + \frac{1}{5} C_3 - \frac{26}{105} C_4 - \frac{1}{70} C_5$$

and the difference is

$$\rho_\parallel - \rho_\perp = \frac{2}{5} C_1 + \frac{3}{10} C_2 + \frac{12}{35} C_4 + \frac{3}{70} C_5.$$

Neglect, for the moment, terms in

$$\rho_{ij} = a_{ij} + a_{ijk} \alpha_k + a_{ijkl} \alpha_k \alpha_l + \cdots$$

that are higher than quadratic in the α_i. Then

$$\rho_\parallel - \rho_{\text{demag}} = 2\delta$$
$$\rho_\perp - \rho_{\text{demag}} = -\delta$$

where

$$\delta \equiv \frac{2}{15} a_{1111} - \frac{2}{15} a_{1122} + \frac{1}{5} a_{2323}.$$

From the viewpoint of symmetry δ could be of either sign. If δ is positive, then $\rho_\parallel > \rho_\perp$ as almost always is the case, experimentally. However, the resistivity as a function of applied field shown in Fig. 1b indicates that this early truncation of the ρ_{ij} series is not always justified, because $\rho_\parallel - \rho_{\text{demag}}$ is unequal to 2δ.

B. Microscopic Theory

In this section, the ferromagnetic resistivity anisotropy is considered from a microscopic, quantum-theory point of view. The form that the results of such calculations must take is discussed in the previous section (IIA). Here, we are interested in the sign and magnitude of the effect.

It is convenient at this point to think in terms of conductivity rather than resistivity, because the basic quantity of interest is the current density J that exists due to an applied force $-e(E + v \times B)$ on the electrons. The ith component of J can be written as

$$J_i = \sigma_{ij}(B) E_j$$
$$= -e \sum_{\text{all electrons}} v_i$$
$$= -\frac{e}{8\pi^3} \sum_n \int v_i(k) f_n(k) \, d^3k \tag{4}$$

where $f_n = f_n^0 + f_n^1$ is the Fermi distribution function for the nth band, written in terms of the equilibrium distribution function f^0 and a small correction f^1. There are as many f_n in the problem as there are partially filled bands. These functions are solutions to Boltzmann's equation, which demands that in the steady state the time rate of change of f_n due to the applied force is cancelled by that due to collisions. These collisions are the basis of the finite conductivity and are worth a short digression.

In the one-electron picture of metals, each electron moves in the periodic potential of the lattice and the *average* potential of all other electrons. The solutions to Schroedinger's equation for this potential are stationary states $\psi_{n,k}$ which, by definition, have infinite lifetime and consequently lead to infinite conductivity. Deviations from perfect periodicity of the lattice caused by phonons, impurities, grain boundaries, etc., allow an electron initially in the state $|n, k\rangle$ to be found later in a state $|n', k'\rangle$. Thus, the word "collision" means any interaction or scattering mechanism that causes transitions between the single-particle states and not, in the usual treatment of resistivity, a collision between two electrons. (But electron–electron interactions can be considered in the context of improving upon the average potential assumption—i.e., correlation effects.)

The calculation of $\sigma_{ij}(B)$ would of course be straightforward if the $f_n(k)$ were known. Unfortunately, the $f_n(k)$ are solutions to N coupled nonlinear integro-differential equations

$(n = 1, 2, \cdots, N)$ of the form

$$-\frac{e}{\hbar}(E + v \times B) \cdot \nabla_k f_n(k) = \sum_{n', k'} \{ [1 - f_n(k)] f_{n'}(k')$$
$$\cdot P_{k',k}^{n'n} - [1 - f_{n'}(k')] f_n(k) P_{k,k'}^{nn'} \} \tag{5}$$

where the sum over states $|n', k'\rangle$ is such that energy is conserved and where the P's are transition probabilities. These in turn are proportional to the squared modulus of the perturbation potential matrix element connecting initial and final states multiplied by the density of final states. This is the Born approximation, valid to the extent that the perturbation potential is small. Scattering due to impurities located far from the host on the periodic table cannot be so treated. In this case, a partial wave analysis is required.

Thus, the electronic wavefunctions $\psi_{n,k}$ are needed in order to calculate the transitions probabilities

$$P_{k,k'}^{m,n'} = \frac{1}{4\pi^2 \hbar} \frac{|\langle n', k' | V_{\text{scatt}} | n, k \rangle|^2}{|\nabla_{k'} \epsilon(k')|}$$

that appear in Boltzmann's equation; and, as we shall see, these wavefunctions must reflect the ferromagnetic ordering of the material.

How much of this formidable problem can be discarded while retaining a plausible model of the resistance anisotropy in ferromagnets, capable of predicting with reasonable agreement the results of experiment? Not much, as we shall attempt to show. Suppose we introduce the concept of a relaxation time by rewriting Eq. (5) as

$$-\frac{e}{\hbar}(E + v \times B) \cdot \nabla_k [f_n^0(k) + f_n^1(k)] = -\frac{f_n^1(k)}{\tau_n(k)}.$$

The virtue of τ is that in simple cases it turns out to be a function of $|k|$ and not k, but at any rate $\tau(k)$ ought to be a simpler function than $f_n(k)$. A formal series-solution [56] for f_n can be written down in terms of τ:

$$f_n(k) = f_n^0(k) + e \frac{\partial f^0}{\partial \epsilon} \{ 1 + \tau_n(k)\Omega + [\tau_n(k)\Omega]^2 + \cdots \}$$
$$\cdot \tau_n(k) \, v \cdot E$$

where Ω is the operator

$$\Omega \equiv \frac{e}{\hbar}(v \times B) \cdot \nabla_k$$

and where it is tacitly assumed the series converges, which will be true provided B is not too large. Equations for the $\tau_n(k)$ are obtained by substituting

$$f_n(k) = f_n^0(k) + \frac{\partial f^0}{\partial \epsilon} \tau_n(k) \, v \cdot E$$

back into Eq. (5). Alternatively, substituting the series solution for $f_n(k)$ in terms of $\tau_n(k)$ back into the basic equation for J_i, Eq. (4), gives

$$\sigma_{ij}(B) = \sigma_{ij}^0 + \sigma_{ijk}^1 B_k + \sigma_{ijkl}^2 B_k B_l + \cdots \tag{6}$$

where

$$\alpha_{ij}^0 \propto \int \tau \frac{v_i v_j}{|v|} \, ds$$

and where the elements of the higher rank tensors $\sigma_{ijk}^{(1)}$, etc., depend to an increasing degree on the topography of the Fermi surface. In ordinary metals the first term in $\sigma_{ij}(B)$ [Eq. (6)] is the zero-field conductivity and the third term the magnetoconductance (or magnetoresistance) effect.

As an example, consider two spherical overlapping bands, each characterized by number of electrons n_i, constant relaxation times τ_i, and effective mass m_i^* where $i = 1$ or 2 is the band index. Take B along the z axis. Then, upon calculating the conductivity tensor and its matrix inverse, the diagonal elements

$$\rho_{xx} = \rho_{yy} = \frac{1}{\sigma_1 + \sigma_2} + \frac{\sigma_1 \sigma_2}{(\sigma_1 + \sigma_2)^3}(\omega_1 \tau_1 - \omega_2 \tau_2)^2$$

and

$$\rho_{zz} = \frac{1}{\sigma_1 + \sigma_2}$$

are obtained, where

$$\sigma_i = \frac{n_i e^2 \tau_i}{m_i^*}$$

and where $\omega_i = eB/m_i^*$ is the cyclotron frequency. As expected $\rho_\perp \equiv \rho_{xx}$ (or ρ_{yy}) is greater than $\rho_\parallel \equiv \rho_z$. Magnetoresistance is also obtained for a single band provided the Fermi surface is sufficiently convoluted. Both cases are examples of the ordinary magnetoresistance effect, obtained by assuming constant, isotropic, relaxation times, and are appreciable only when the $\omega\tau$ products are not small, a situation favored by sample purity, low temperature, and high magnetic field.

Kohler's rule is satisfied by the two-band example *if* it is assumed that $\tau_1 = \tau_2 \equiv \tau$. Then

$$\frac{\Delta\rho}{\rho_0} \propto B^2 \tau^2 e^2 \left(\frac{1}{m_1} - \frac{1}{m_2}\right)^2$$

$$= \text{const} \times (B/\rho_0)^2$$

and

$$\ln\left(\frac{\Delta\rho}{\rho_0}\right) = 2 \ln(B/\rho_0) + \text{const.}$$

The concept of an effective field (not the Weiss field) arises for ferromagnets by writing

$$B = H_{\text{applied}} + \alpha 4\pi M$$

and determining α from the Kohler diagram; however the justification is lacking.

The expression [Eq. (6)] for $\sigma_{ij}^{(0)}$ indicates perhaps better than any other that the starting point of a conductivity calculation is some assumptions about, or calculations for, the energy bands $\epsilon_n(k)$. These define the Fermi surface and give the velocity

$$v_n(k) = \frac{1}{\hbar} \nabla_k \epsilon(k)$$

associated with each state $|n, k\rangle$. The need for the wavefunctions is subtly disguised in $\tau(k)$. The energy bands for ferro-

magnetic Ni according to Connolly's self-consistent $x\alpha$-method calculation [57] are shown in Fig. 13a and are typical of those for the ferromagnetic transition series metals in several ways.

These metals are characterized by the filling of relatively narrow d bands capable of holding a total of 10 electrons per atom, thus the associated density of states is very large. The d bands are relatively flat, causing the elements of the effective mass tensor

$$m_{ij}^* = \hbar^2 \left[\frac{\partial^2 \epsilon(k)}{\partial k_i \partial k_j}\right]^{-1}$$

to be large. This, in turn, means that the mobility of d electrons is low. Cutting through and hybridized with the d bands is a broad s-p band from the $4s$ atomic level. This hybridization makes it incorrect, strictly speaking, to talk about separate s and d bands but at the point where the Fermi level crosses there are two classes of electron states with very different properties (Fermi velocity and effective mass) and therefore the terminology is retained. The net magnetic moment is explained by exchange-split d bands with the s-p band remaining essentially spin-degenerate.

It was usually assumed that the effect of alloying, for example, Ni with Cu is simply to shift the Fermi level with the
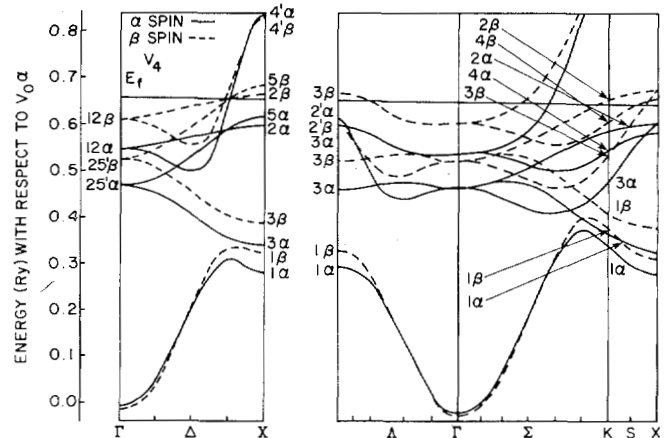

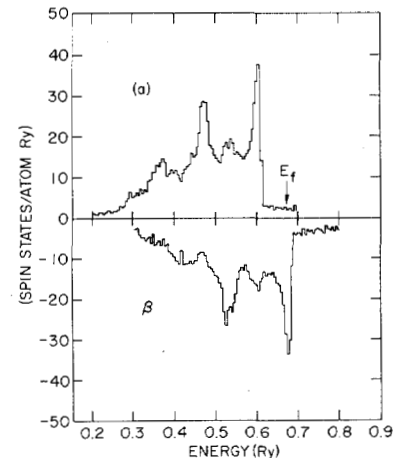Fig. 13a. Band structure of nickel (Connolly [57]).

Fig. 13b. Calculated density of states for minority- and majority-spin electrons in ferromagnetic Ni (Connolly [57]).

bandstructure remaining fixed. According to this rigid band approximation the size of the d electron (or d hole, since the effective mass is negative) Fermi surfaces would shrink. Just prior to disappearing they would be ellipsoids centered at the symmetry points $X[k = (\pm 2\pi/a, 0, 0), (0, \pm 2\pi/a, 0),$ and $(0, 0, \pm 2\pi/a)]$. The rigid band approximation for these alloys is based more on desire than fact, because photoemission studies [58] give it little support. Instead, they show that the density of states curve is roughly the sum of those for the constituents and support the existence of two separate sets of bands.

Mott [4], [59] first pointed out that in the $3d$ metals, specifically Ni, most of the current is carried by s electrons because m_d^* is large, and that interband (sd) transitions make the dominant contribution to the resistivity because $N_d(\epsilon_F)$ is large. Of course, a large m_d^* implies a large $N_d(\epsilon_F)$ if the bands are spherical and parabolic as Mott assumes. This simplifying assumption allows him to solve the two coupled Boltzmann equations in the relaxation time approximation, obtaining two constant, isotropic, relaxation times τ_s and τ_d. He obtains, approximately,

$$\frac{1}{\tau_s} = \int P_{k,k'}^{sd} \, ds'$$
$$= \frac{\pi}{\hbar} N_d(\epsilon_F) \int \left| V_{k,k'}^{sd} \right|^2 \sin \theta' \, d\theta' \qquad (7)$$

where θ' is the angle between k and k'. The conductivity is simply

$$\sigma = \frac{n_s e^2 \tau_s}{m_s^*}.$$

where m_s^* is approximately the free electron mass and τ_s is inversely proportional to $N_d(\epsilon_F)$. Mott's model not only explains the relatively high resistivity of Ni, but also the decrease in resistivity upon ferromagnetic ordering: The d bands split with the majority spin bands entirely below the Fermi level, causing a decrease in $N_d(\epsilon_F)$.

Another simplification results by recognizing that the majority and minority spin s electrons independently contribute to the conductivity whenever spin is conserved in the scattering process, which is the case when the scattering potential does not depend on spin (phonons, impurities, etc.). This is sometimes referred to as the "two-current" model and should be a good approximation at temperatures well below the Curie temperature where the number of magnons is negligible. Thus

$$\sigma = \sigma_{s+} + \sigma_{s-}$$

where "$+$" refers to minority spin electrons and "$-$" to majority spins. The sign denotes the electronic spin and not the antiparallel magnetic moment.

Yet another plausible simplification results by assuming that the probabilities of sd scattering and ss scattering are additive. This is tantamount to solving the coupled equations for f_n (or τ_n) for limiting cases, first when sd scattering is dominant and next when ss scattering is dominant (as it is when $N_d(\epsilon_F) \simeq 0$), and writing for the intermediate case

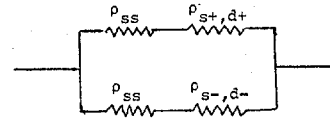$$\frac{1}{\tau} = \frac{1}{\tau_{ss}} + \frac{1}{\tau_{sd}}.$$

When combined with the two-current model this gives

$$\sigma = \frac{ne^2}{m_s} \left[\frac{1}{\dfrac{1}{\tau_{ss}} + \dfrac{1}{\tau_{s+,d+}}} + \frac{1}{\dfrac{1}{\tau_{ss}} + \dfrac{1}{\tau_{s-,d-}}} \right]$$

where $n \equiv n_{s+} = n_{s-}$ and $\tau_{ss} \equiv \tau_{s+,s+} = \tau_{s-,s-}$. It is expected that $\tau_{s+,d+}$ and $\tau_{s-,d-}$ will be different because the d bands are exchange split. This formula can be schematically rewritten as

$$\frac{1}{\rho} = \frac{1}{\rho_{ss} + \rho_{s+,d+}} + \frac{1}{\rho_{ss} + \rho_{s-,d-}}$$

which is the resistivity of the following network:

According to Mott's model the conductivity of Ni increases upon ferromagnetic ordering because the density of available majority-spin d states becomes zero; therefore $P_{s-,d-} = 0$ and $\rho_{s-,d-} = 0$. Only the zero-field conductivity $\sigma_{ij}^{(0)}$ is considered, and the magnetic moment enters only as a consequence of exchange-split d bands. The conductivity is isotropic because the bands are assumed to be isotropic.

If sd scattering is the dominant feature of transition-metal electronic conductivity, then the ferromagnetic resistance anisotropy must be a consequence of an anisotropic scattering mechanism. This could result from some lower-than-cubic-symmetry scattering potential (e.g., magnons) with cubic-symmetry initial and final states, or from an isotropic scattering potential with lower-than-cubic-symmetry wavefunctions. The latter mechanism is generally considered the more likely one. The symmetry of the wavefunctions is lowered by the spin-orbit interaction, which was proposed by Brooks [60] as an explanation of magnetocrystalline anisotropy and by Smit [3] as an explanation of the resistance anisotropy in ferromagnets. The spin-orbit interaction has the form

$$H_{\text{s.o.}} = K L \cdot S$$

provided the electrostatic potential is radial. It makes a contribution to the energy of the d states that depends on spin or magnetization direction, making it favorable for the magnetization to point along certain crystalographic directions. Thus the d electron spin is coupled to its orbital motion, which in turn is coupled to the lattice by the crystal field. If M is constrained along a particular crystallographic direction, then the techniques of quantum mechanics can be used to calculate new wavefunctions ψ_d^1 in terms of the ψ_d^0 that are obtained when the spin-orbit interaction is neglected. The ψ_d^1 exhibit symmetry lower than cubic and are not eigenfunctions of S_z because the spin-orbit interaction mixes states of opposite spin. Therefore, both

$$\frac{1}{\tau_{s+,d}} \simeq \frac{2\pi}{\hbar} N_d(\epsilon_F) \left| \int \psi_{s+}^* V_{\text{scatt}} \psi_d^1 \, d\tau \right|^2$$

and

$$\frac{1}{\tau_{s-,d}} \simeq \frac{2\pi}{\hbar} N_d(\epsilon_F) \left| \int \psi_{s-}^{*} V_{\text{scatt}} \psi_d^1 \, d\tau \right|^2$$

exhibit symmetry lower than cubic. Here, $d\tau$ denotes an integration over both spatial and spin coordinates and the k' dependence of $|V_{k,k'}^{sd}|^2$ appearing in Eq. (7) is ignored for simplicity. A separate spherical parabolic s band is invariably assumed, with

$$\psi_s = e^{ik \cdot r} \chi$$

where χ is a spin function. Generally, $V_{\text{scatt}}(r)$ is assumed to be radial, such as

$$V_{\text{scatt}} = \frac{\Delta Z e^2}{r} e^{-qr}$$

where q^{-1} is a screening length. Under these conditions, the zero-field conductivity tensor is

$$\sigma_{ij}^0 = \frac{ne^2}{m_s} \left[\frac{3}{4\pi k_f^4} \int \frac{k_i k_j \, ds}{\dfrac{1}{\tau_{ss}} + \dfrac{1}{\tau_{s+,d}(k)}} \right.$$
$$\left. + \frac{3}{4\pi k_f^4} \int \frac{k_i k_j \, ds}{\dfrac{1}{\tau_{ss}} + \dfrac{1}{\tau_{s-,d}(k)}} \right]$$

where k_f is the Fermi wavenumber for s electrons and ds denotes an integration over the spherical Fermi surface in k space.

Further progress requires some work. It is necessary to

(a) choose plausable ψ_d^0,

(b) specify M,

(c) compute ψ_d^1,

(d) evaluate the integral over k' in Eq. (7) for $\tau_{s\pm,d}$, and,

(e) evaluate the conductivity integrals.

The magnetization is generally, but not always, assumed to lie along a crystallographic axis. Beyond this, however, the paths of the calculations reported in the literature show considerable divergence. Smit [3], in the original calculation, chooses the ψ_d^0 as exchange—and crystal-field-split atomic $3d$ levels with wavefunctions $xy f(r)$, etc. He discards the $L_z S_z$ term in $L \cdot S$ and calculates the ψ_d^1 via nondegenerate first-order perturbation theory. Because he considers only the scattering of majority-spin electrons he is interested in ψ_d^1 of the form (in our notation where the superscripts are opposite in sign to those of Smit [3]):

$$\psi_d^1 = \phi_d \chi^+ + \frac{K}{2\gamma} \sum_{d'} b_{d'} \phi_{d'} \chi^-$$

where ϕ_d are the atomic orbitals, K the spin-orbit coupling parameter, 2γ the exchange splitting, and $b_{d'}$ the numerical coefficients that arise from the actual perturbation-theory calculation. In Smit's calculation these coefficients are such that the sum of the five ψ_d^1 contains a *deficit* of orbitals of the type

$$xy f(r) \chi^-$$

and

$$\tfrac{1}{2}(x^2 - y^2) f(r) \chi^-.$$

The significance of this is that majority-spin s electrons traveling parallel to the magnetization have the highest probability of scattering. This follows because if the scattering potential is spherically symmetrical, then its matrix elements have the form

$$\int xy f(r) V_{\text{scatt}}(r) e^{ik \cdot r} d^3 r \propto k_x k_y$$

and

$$\tfrac{1}{2} \int (x^2 - y^2) f(r) V_{\text{scatt}}(r) e^{ik \cdot r} d^3 r \propto \tfrac{1}{2}(k_x^2 - k_y^2)$$

which are both zero if $k_x = k_y = 0$. Thus electrons traveling along the z axis do *not* scatter into these states. However, Smit's calculation shows a *deficit* of these two states; therefore the sd scattering probability is greatest for electrons traveling parallel to the magnetization (or z axis), and $\rho_\parallel > \rho_\perp$ as experimentally observed. The result $\rho_\parallel > \rho_\perp$ also is obtained by Berger [61], who considers only the term $L_z S_z$ in $L \cdot S$.

Smit also observes that if the scattering potential is non-spherical, as would be the case for ions displaced from their lattice sites (phonons) and for grain boundaries, then the anisotropy in the matrix elements will be reduced. This leads to a temperature-dependent resistivity anisotropy ratio

$$\frac{\Delta \rho}{\rho} = \frac{n_{\text{imp}} \Delta \rho_{0,\text{imp}} + \langle n_{\text{ph}}(T) \rangle \Delta \rho_{0,\text{ph}}}{n_{\text{imp}} \rho_{0,\text{imp}} + \langle n_{\text{ph}}(T) \rangle \rho_{0,\text{ph}}}$$

where $\langle n_{\text{ph}} \rangle$ is the number of phonons at temperature T and $\rho_{0,\text{imp}}$ and $\rho_{0,\text{ph}}$ are contributions from the two different scattering mechanisms. Consequently, $\Delta \rho / \rho$ is expected to increase with decreasing temperature, to be insensitive to impurity concentration changes when $n_{\text{imp}} \gg \langle n_{\text{ph}}(T) \rangle$, and to show a dip at alloy concentrations permitting ordered structures (e.g., $Ni_3 Fe$) and for pure elements.

In a recent calculation by Potter [62], the d electrons are assumed to form a band and all terms in $L \cdot S$ are retained. The spatial part of the ψ_d^0 is, according to the tight-binding method,

$$\psi_{n,k}^0 = \sum_{l,m} e^{ik \cdot R_l} a_{n,m}(k) \phi_m(r - R_l)$$

where the ϕ_m, $m = 1, 2, \cdots, 5$ are atomic orbitals. The coefficients $a_{n,m}(k)$ depend on the crystal structure and have been worked out for Ni by Fletcher [63] at points of high symmetry within the Brillouin zone. The d bands are assumed to be uniformly exchange split with this and other relevant energy separations taken from Conolly's [57] self-consistent calculations, Fig. 13b. The ψ_d^1 wavefunctions are worked out by noting that the spin-orbit operator has the periodicity of the lattice and hence is diagonal in k. The integration over k' that appears in Eq. (7) for τ_{sd} is avoided by assuming the d bands are nearly full, as is the case for Ni, and approximating k' by the points X at the top of the band. Terms with large (greater than about 2 eV) energy denominators are neglected in calculating the ψ_d^1, and hence only the energy splittings ϵ

and 2γ enter the problem, where ϵ is the splitting between the uppermost two d bands of like spin at X and 2γ the exchange splitting, assumed uniform. The results of the calculations for $\tau_{s+,d}$ and $\tau_{s-,d}$ are

$$\frac{1}{\tau_{s+,d}} = \frac{4\pi}{\hbar} C_{sd}^2 N_d \left\{ k_y^2 k_z^2 + k_z^2 k_x^2 + k_x^2 k_y^2 \right.$$
$$+ \frac{1}{96}\left(\frac{K}{\epsilon}\right)^2 [(k_y^2 - k_z^2)^2 + (k_z^2 - k_x^2)^2 + (k_x^2 - k_y^2)^2]$$
$$\left. + \frac{1}{96}\left(\frac{K}{\epsilon}\right)^2 (2k_z^2 - k_x^2 - k_y^2)^2 \right\}$$

and

$$\frac{1}{\tau_{s-,d}} = \frac{4\pi}{\hbar} C_{sd}^2 N_d \left\{ \frac{1}{16}\left(\frac{K}{2\gamma}\right)^2 (k_y^2 k_z^2 + k_z^2 k_x^2 + k_x^2 k_y^2) \right.$$
$$+ \frac{1}{6}\left[\frac{1}{8} + \left(\frac{1-\sqrt{6}}{16}\right)^2\right]\left(\frac{K}{2\gamma+\epsilon}\right)^2$$
$$\cdot [(k_y^2 - k_z^2)^2 + (k_z^2 - k_x^2)^2 + (k_x^2 - k_y^2)^2]$$
$$- \frac{1}{6}\left[\frac{1}{16} - \left(\frac{1-\sqrt{6}}{16}\right)^2\right]\left(\frac{K}{2\gamma+\epsilon}\right)^2 (2k_z^2 - k_x^2 - k_y^2)^2$$
$$\left. - \frac{1}{32}\left(\frac{K}{2\gamma}\right)^2 (k_x^2 + k_y^2) k_z^2 \right\}.$$

Each τ consists of a cubic symmetry, a $\cos^2\theta$, and a $\cos^4\theta$ term. Contrary to Smit's calculation, this one indicates that

$$\frac{1}{\tau_{s-,d}\,(\theta = 0)} < \frac{1}{\tau_{s+,d}\left(\theta = \frac{\pi}{2}\right)}$$

which implies $\rho_\parallel < \rho_\perp$ if the anisotropy is due to majority-spin electrons. However,

$$\frac{1}{\tau_{s+d}\,(\theta = 0)} > \frac{1}{\tau_{s+d}\left(\theta = \frac{\pi}{2}\right)}$$

which suggests that the condition $\rho_\parallel > \rho_\perp$ is due to the scattering of minority-spin electrons.

The conductivity integrals are of the form

$$\sigma_\parallel^+ \propto \frac{1}{N_d}\int \frac{k_z^2 k_f^2 \sin\theta\, d\theta\, d\phi}{k_y^2 k_z^2 + k_z^2 k_x^2 + k_x^2 k_y^2 + k_f^4\left[\left(\frac{K}{\epsilon}\right)^2 f(\theta,\phi) + \beta\frac{N_s}{N_d}\right]}$$

where the sought after ferromagnetic resistivity anisotropy resides in $f(\theta,\phi)$ and $\beta(N_s/N_d)$ is a term due to isotropic ss scattering. Upon evaluation of these integrals with certain approximations discussed in ref. (62), the result

$$\frac{\Delta\rho}{\rho_{av}} = \frac{\rho_\parallel - \rho_\perp}{\frac{1}{3}\rho_\parallel + \frac{2}{3}\rho_\perp} = \frac{3(\sigma_\perp - \sigma_\parallel)}{\sigma_\perp + 2\sigma_\parallel}$$

where

$$\sigma_\parallel = \sigma_0 \left\{ 1 - \frac{1}{140\beta}\frac{N_d}{N_s}\left[\left(\frac{K}{2\gamma}\right)^2 + \frac{5+2\sqrt{6}}{24}\left(\frac{K}{2\gamma+\epsilon}\right)^2\right] \right.$$
$$\left. - \frac{3\sqrt{3}\beta}{2}\frac{N_s}{N_d}\ln\left[\frac{1}{16}\left(\frac{K}{\epsilon}\right)^2 + \beta\frac{N_s}{N_d}\right]\right\}$$

and

$$\sigma_\perp = \sigma_0 \left\{ 1 - \frac{1}{140\beta}\frac{N_d}{N_s}\left[\frac{5}{4}\left(\frac{K}{2\gamma}\right)^2 + \frac{19-2\sqrt{6}}{8}\left(\frac{K}{2\gamma+\epsilon}\right)^2\right] \right.$$
$$\left. - \frac{3\sqrt{3}\beta}{2}\frac{N_s}{N_d}\ln\left[\frac{1}{32}\left(\frac{K}{\epsilon}\right)^2 + \beta\frac{N_s}{N_d}\right]\right\}$$

is obtained. Due to the approximations these expressions are applicable only when the second terms and the arguments of the logarithms are small compared to unity. Note that the conductivity integrals diverge if ss scattering is neglected.

In Potter's calculation, $\Delta\rho/\rho_{av}$ turns out to be a function of four parameters: $\beta N_s(\epsilon_F)/N_d(\epsilon_F)$, K/ϵ, $K/2\gamma$, and $K/(2\gamma+\epsilon)$. The significance of $\beta N_s/N_d$ is that it gives the relative importance of isotropic ss scattering and anisotropic sd scattering. As to the sign of $\Delta\rho/\rho_{av}$, there is competition between minority and majority spin scattering as discussed before and $\Delta\rho/\rho_{av}$ can be of either sign depending on the actual values of the four parameters. The most interesting parameter is K/ϵ; first because $\Delta\rho/\rho_{av}$ is large and positive for large K/ϵ, and second because the bands separated by ϵ at X actually cross along Δ (the coordinate axes), and this happens very near the Fermi level for pure Ni. This degeneracy is, of course, removed upon departing from Δ, but nevertheless the splitting will not be great. It seems likely that this feature and not the large density of d states per se produces a large, positive $\Delta\rho/\rho$ in alloys of Ni. Berger [61] has made a similar observation.

An estimate for $Ni_{0.7}Cu_{0.3}$ is $N_d/\beta N_s = 14$ and $\Delta\rho/\rho_{av} = 0.44\%$, based on Connolly's band splittings, and $K = 0.1$ eV, [64]: $K/\epsilon = \frac{1}{3}$, $K/2\gamma = \frac{1}{8}$, and $K/(2\gamma+\epsilon) = \frac{1}{11}$. A single rigid band structure is assumed which for Ni-Cu is not really the case.

III. EXPERIMENTAL RESULTS

A. Bulk Materials

We have chosen to present the available data on anisotropic magnetoresistance in a series of tables that are divided into elements (I), binary alloys and compounds (II), ternary alloys and compounds (III), and films (IV). Listed on each table are a series of comments that clarify the particular measurement.

A comprehensive survey of the literature reveals that very few compounds or alloy systems have been investigated. Smit [3] and van Elst [10] are the largest contributors. Although magnetoresistance has been extensively studied in magnetic materials, the resistivity anisotropy is seldom reported. For example, several conducting spinels have been studied, but only for magnetite [68] is the anisotropic magnetoresistance given.

Methods for plotting the data so as to give the greatest understanding are of interest. One possibility is to plot $\Delta\rho/\rho_{av}$ as a function of composition as shown for Ni-Fe and Ni-Co in Figs. 2 and 3. Another, following Snoek [11], is to emphasize the filling of electron energy bands by modifying the horizontal axis of Figs. 2 and 3 to show the number of electrons n_d associated with the $3d$ band or the closely related parameter, the mean Bohr magneton number n_B (as obtained from the saturation magnetization.) In the simple case of a filled spin up band and a nearly filled spin down band, $n_B = 10 - n_d$.

TABLE II
Binary Alloys

Alloy	Temp °K	$\Delta\rho/\rho_0$ %	ρ_0 μΩcm	$\Delta\rho$ μΩcm	$4\pi M^*$ G	n_B^*	T_c^* °K	Ref	Comment
$NiC_{.0013}$	4.2	1.67	.45	.0075	6300	.6	630	65	b
$NiCr_{.0017}$	4.2	-.23	.86	-.002	6300	.6	630	65	
Fe_7Se_8	300	06							
	150	-.33					450	66	c
MnP	4.2 to 50	0.0						67	d
Fe_3O_4	300	<0.2	~7500		6100	4	850	68	
$Fe_{.9}V_{.1}$	273	1.3			19400	1.9	1100	69	Fig. 21
	77	7.5							
	4.2	8.5							
$Ni_{.80}Co_{.20}$	293	6.5	11.3	.72	8700		870	10	e
	77	16.4	3.9	.64					
	14	20.0	.6	.60	9000	.86			
$Ni_{.76}Fe_{.24}$	293	3.8	13.3	.50	11300		873	10	e
	77	10.8	5.0	.54					
	14	12.7	4.2	.54	12200				
$Ni_{.83}Pd_{.17}$	293	2.3	9.7	.22			598	10	
	77	2.1	2.8	.064					
	14	1.7	2.0	.036		.60			
$Ni_{.69}Pd_{.31}$	293	2.0	12.3	.25			568	10	
	77	2.6	4.8	.12					
	14	2.4	4.0	.09		.60			
$Ni_{.99}Cr_{.01}$	293	.79	17.4	.14			598	10	f
	77	.11	8.9	.01					
	14	-.01	7.8	-.001	6100	.55			
$Ni_{.937}Cr_{.063}$	293	-.01	64.7	-.001			323	10	f
	77	-.18	52.2	-.09					
	14	-.24	49.5	-.12	2600	.29			
$Ni_{.97}Si_{.03}$	293	.10	21.0	.02	3300		425	10	f
	77	2.4	13.2	.32					
	14	2.6	11.6	.30	4000	.39			
$Ni_{.94}Sn_{.06}$	293	1.8	17.5	.32			533	10	f
	77	3.3	8.6	.28					
	14	3.4	7.2	.24	4200	.40			
$Ni_{.96}Al_{.04}$	293	.85	27.7	.23			398	10	f
	77	3.4	19.1	.65					
	14	3.9	17.7	.69	3900	.37			
$Ni_{.97}V_{.03}$	293	.54	26.0	.13			473	10	f
	77	.63	18.2	.11					
	14	.60	17.6	.10	4200	.40			

Alloy	Temp °K	$\Delta\rho/\rho_0$ %	ρ_0 μΩcm	$\Delta\rho$ μΩcm	$4\pi M^*$ G	n_B^*	T_c^* °K	Ref	Comment
$Ni_{.98}Mn_{.02}$	293	2.9	15.0	.44			613	10	f
	77	7.2	8.3						
	14	9.9	2.3	.23	6500	.64			
$Ni_{.94}Mn_{.06}$	293	2.5	19.7	.49			573	10	f
	77	7.1	9.1	.64					
	14	8.8	7.2	.62	6800	.72			
$Ni_{.95}W_{.05}$	293	1.04	16.7	.17			513	10	f
	77	1.01	11.0	.11					
	14	.83	10.7	.09	2400	.27			
$Ni_{.95}Mo_{.05}$	293	.34	28.3	.10	2500		463	10	f
	77	.21	20.0	.06					
	14	.07	18.3	.01	3700	.35			
$Ni_{.90}Zn_{.05}$	293	2.6	12.2	.31	4500		340	10	f
	77	5.0	5.2	.17					
	14	5.7	4.6	.26	5000	.50			
$Ni_{.99}Fe_{.01}$	RT	2.7	8.85	.24	6300		643	[70]	
	77	5.9	1.45	.086					
	4.2	5.9	.707	.042	6600	.62			
$Ni_{.978}Fe_{.022}$	RT	3.0	12.09	.36	6600		655	[70]	
	77	7.9	2.02	.16					
	4.2	10.6	.92	.098	7000	.65			
$Ni_{.917}Fe_{.083}$	RT	5.4	12.92	.70	7900		716	[70]	
	77	13.1	4.26	.56					
	4.2	14.9	3.49	.52	8400	.78			
$Ni_{.83}Fe_{.17}$	RT	4.3	14.9	.64	9800		805	[70]	
	77	14.4	5.35	.77					
	4.2	16.4	4.75	.78	10600	.98			
$Ni_{.994}Co_{.006}$	RT	2.1	8.1	.19	6100		633	[20]	
	77	3.5	1.2	.044					
	4.2	3.8	.60	.023	6500	.60			
$Ni_{.975}Co_{.025}$	RT	3.0	8.8	.26	6400		665	[20]	
	77	6.7	1.6	.11					
	4.2	8.7	.81	.07	6800	.63			
$Ni_{.946}Co_{.054}$	RT	3.6	10.7	.38	6700		700	[20]	
	77	8.6	2.8	.24					
	4.2	10.6	2.2	.23	7100	.66			
$Ni_{.893}Co_{.107}$	RT	4.9	11.1	.55	7400		760	[20]	
	77	9.6	3.0	.39					
	4.2	16.2	2.0	.32	7700	.75			
$Ni_{.70}Co_{.30}$	RT	6.6	11.3	.75	9900		950	[20]	
	77	21.0	4.0	.84					
	4.2	26.7	3.1	.84	10200	.97			

[b]Data are given for nickel with carbon solutes from 5 to 8000 pp. The data are analyzed in terms of the anisotropic effect and the normal (Lorentz force) magnetoresistance. Angular dependence is studied, showing that demagnetizing effects can cause anomalous behavior at low fields. Several Kohler plots are given.

[c]The values of $\Delta\rho/\rho_0$ are based on transverse resistivity measurements made in fields of 12.5 kG. A change in magnetic order at 200°K is speculated.

[d]Hall effect is positive for phosphor concentrations from 33 to 53%. Both $\Delta R_{\parallel}/R$ and $\Delta R_{\perp}/R$ as a function of H were negative and of the same magnitude.

Fig. 21. This figure shows data for a range of compositions of Fe-V (Sueda and Fujiwara [67]).

[e]The data given by van Elst [10] and Smit [3] for Ni-Fe and Ni-Co as shown in Fig. 3 are for the anisotropic ratio ($\Delta R/R$) only and are not listed in the table.

[f]Several compositions of this binary alloy are listed by van Elst [10]. In all cases, except for Mn and Cu, there is a decrease in $\Delta\rho/\rho$ with increased concentration of the solute element in nickel.

Data are shown in Figs. 14a and 14b for several alloy systems at 20°K plotted against n_B. The outstanding feature of these plots is that, with the exception of the pure elements and ordered compounds, the data form a smooth curve peaking at approximately 0.9 n_B. One reason for the exception is discussed in Section II B.

The maximum at about 0.9 n_B is often attributed to a peaking in the density of states at this composition. However, it is known from photoemission data [30] that for the maximum value of $\Delta\rho/\rho_{av}$ the Fermi level is not at the peak in the density of states curve. For example, the Fermi level for pure Ni, as determined both theoretically [57] and as inferred from
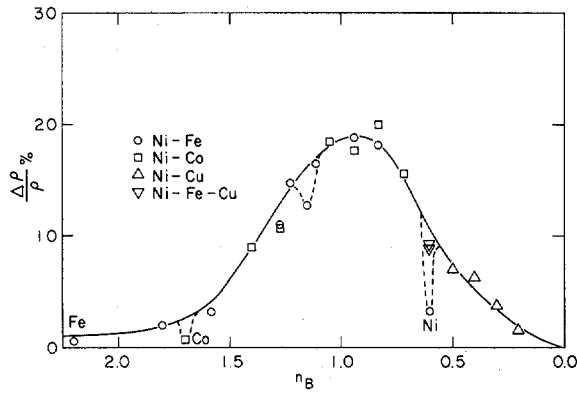
Fig. 14a. Anisotropic magnetoresistivity ratio at 20°K plotted against n_B, the average Bohr magneton number for various alloys and elements (Smit [3]).
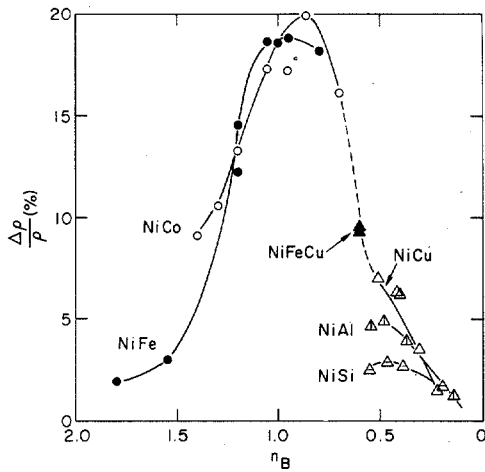

Fig. 14b. Anisotropic magnetoresistivity ratio at 20°K plotted against number of Bohr magnetons, n_B, for Ni-Co (o), Ni-Fe (•), Ni-Cu (△), Ni-Fe-Cu (▲), Ni-Al (△), Ni-Si (△), and Ni-Zn (x) (Van Elst [10]).
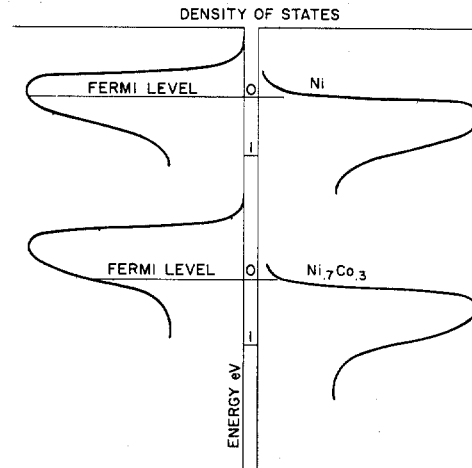
electronic specific heat measurements in Ni alloys [30], is very near the peak in the density of states curve (Figs. 13b and 15), yet the maximum value of $\Delta\rho/\rho_{av}$ in NiCo alloys occurs at 20 to 30 at% Co with the Fermi level far from a peak (Fig. 15). Thus, there is no obvious correlation of the Fermi level with $\Delta\rho/\rho_{av}$. Both Berger [61] and Potter [62] have indicated that the cause is more complex. Of importance in producing a large, positive $\Delta\rho/\rho_{av}$ is the ratio K/ϵ, where K is the spin orbit coupling parameter and ϵ is the splitting between the uppermost two d bands of like spin.

Potter's theory [62] also takes account of certain cases where the sign of $\Delta\rho$ is negative. As discussed in Section II the sign of $\Delta\rho$ depends on whether the electronic conduction is dominated by the scattering of spin up or spin down electrons. From Table II it is seen that Ni-Cr alloys have negative $\Delta\rho$ even at room temperature for the 6% Cr composition. This alloy system may represent the nearly filled $3d$ bands originally described by Potter for the Ni-Cu alloys. In the case of almost filled bands there is a nearly balanced competition of the up and down carriers and small changes in the energy band parameters could shift the sign of $\Delta\rho$. A second alloy

Fig. 15. Schematic of density of states for Ni and $Ni_{0.7}Co_{0.3}$ showing exchange splitting increase and proposed Fermi level shift (McGuire et al. [30]).

TABLE III
Ternary Alloys

Alloy	Temp °K	Δρ/ρ₀ %	ρ₀ μΩcm	Δρ μΩcm	4πM* G	nB*	Tc* °K	Ref	Comment
$Ni_{.69}Fe_{.16}Cu_{.14}$	20	3.30	12.2	.36	8640			71	g
$Ni_{.922}Fe_{.025}$									
$Cu_{.045}$	RT	3.6	14.4	.52				10	
	77	8.3	5.34	.45					
	14	9.5	4.51	.43		.6			
$Ni_{.845}Fe_{.047}$									
$Cu_{.108}$	RT	3.3	19.1	.59				10	
	77	8.2	9.95	.82					
	14	9.2	8.86	.83		.6			
$Ni_{.355}Co_{.496}$	RT	3.3	17.3	.57	11000			70	
$Cu_{.153}$									
$Ni_{.80}Fe_{.163}$	RT	2.2	28.6	.62	10200			70	h
$Mn_{.037}$									
$Ni_{.13}Fe_{.15}Mn_{.11}$	RT	0.4	64	.25	8400			70	h
$Ni_{.24}Co_{.60}Zn_{.17}$	RT	.7	27.8	.20				70	

gValues listed for $Ni_{0.69}Fe_{0.16}Cu_{0.14}$ are deduced from transverse measurements. Hall coefficients over the range 20 to 200°K are given for several compositions of Ni-Fe-Cu.

hThe value of $\Delta\rho/\rho_0$ and $\Delta\rho$ decrease with increasing Mn content in contrast to the film results of Galinier [72].

with negative $\Delta\rho$ is Fe_7Se_8, but this is a case involving a different crystal structure from the fcc Ni-Cr system.

Ternary alloys listed in Table III have anisotropic magnetoresistance values that are not significantly different than binary alloys.

B. Thin Films

Thin films are important because they are used in magnetoresistance devices such as bubble detectors and magnetic recording heads. We have noted in Section I that there are two types of size effects in films. One is related to film thickness
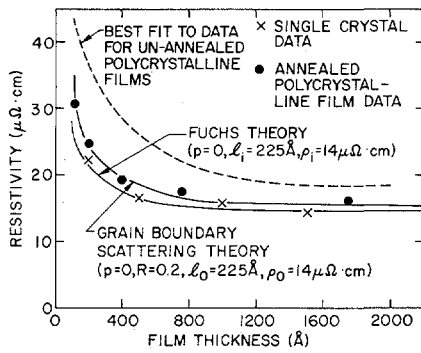
Fig. 16. Resistivity versus film thickness for various permalloy thin films (Mayadas *et al.* [73]).

TABLE IV
Films

Composition	Thickness Å	ρ $\mu\Omega$cm	$\Delta\rho$ $\mu\Omega$cm	$\Delta\rho/\rho$ %	Substrate	Ref
$Ni_{.82}Fe_{.18}$	2515	19.7	.68	3.43	glass	[35]
	1080	17.9	.58	3.23		
	600	21.6	.63	2.97		
	395	23.5	.65	2.75		
	260	28.2	.68	2.56		
	140	34.7	.73	2.10		
	90	39.4	.61	1.56		
$Ni_{.67}Co_{.30}Cr_{.03}$	420	18.2	.76	4.1	Al_2O_3	[70]
	420	16.7	.70	4.1	Si	
	420	17.4	.72	4.1	SiO_2	
	420	43.8	.78	1.7	BeO	
$Ni_{.78}Fe_{.14}Mn_{.08}$ (see comment i)	2000	27.5	1.3	4.2	glass	[72]
$Ni_{.70}Co_{.30}$	300	25.0	.95	3.8	glass	[82]

[i]This paper gives information on a range of Mn from $Ni_{0.81}Fe_{0.16}Mn_{0.03}$ to $Ni_{0.77}Fe_{0.13}Mn_{0.10}$. Values of Hc ($\approx$ 2G.), H_K ($\approx$ 2G.), and λ ($\pm$ 1 $\times$ 10^{-6}) are given. The values of $\Delta\rho$ and $\Delta\rho/\rho_0$ for these films are much larger than bulk values (see Table III).

and the other to grain size. These effects have been studied in $Ni_{0.7}Co_{0.3}$ (Fig. 7). In permalloy both effects are clearly shown in Fig. 16 where Mayadas *et al.* [73] make corrections for grain boundary resistance and also indicate that a permalloy single crystal film fits on the polycrystalline curve that is corrected for grain size. In Fig. 17a and b and Table IV are values of $\Delta\rho$ alone illustrating the important fact that $\Delta\rho$ is independent of thickness. Values of the ratio $\Delta\rho/\rho_{av}$ depend only on ρ_{av}, a result that has not been sufficiently emphasized in the literature.

Several other effects must be examined in thin films to complete our understanding. These include stress, substrate material, inhomogeneities and imperfections, as well as magnetoresistance geometry.

a) *Stress* effects in evaporated films have been studied by Klokholm [28] [74]. One of the specific problems related to magnetoresistance in films used in devices is that they are deposited at elevated temperatures. Films deposited under these conditions have a residual stress at room temperature of two kinds. One kind is the thermal stress caused by the difference in thermal contraction of the film and the substrate. The second kind is an intrinsic stress resulting from the nucleation and growth of crystallites within the film. If the film is magnetostrictive, the residual stress causes changes in the magnetic properties of the film. In particular, magnetic anisotropy and the coercive field are effected. Residual stresses in films can be as high as 10^{10} dynes/cm^2 and can be either tensile or compressive. For permalloy, which has nearly zero magneto-
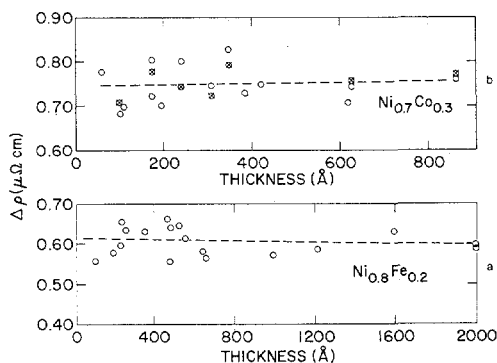

Fig. 17. Anisotropic magnetoresistivity, $\Delta\rho$, as a function of film thickness for (a) $Ni_{0.7}Co_{0.3}$ and (b) $Ni_{0.8}Fe_{0.2}$. Circles with crosses for $Ni_{0.7}Co_{0.3}$ are for annealed films. Resistivities for these films are shown in Fig. 7 (McGuire *et al.* [36]).

striction, the residual stress is not a strong factor in determining the observed magnetic properties.

What effect does stress have on the magnetoresistance? Concerning $\Delta\rho$, we are unaware of investigations in which the effect of stress was systematically studied. However, the response of the film to an applied magnetic field will depend on how the magnetic domains behave when the film is stressed, since it is the magnetization that determines the magnetoresistivity. Thus if the hysteresis loop is modified, the observed resistivity as a function of applied field will be correspondingly changed. Such changes are of importance in any application but do not mean that anisotropic magnetoresistance measured under saturation conditions has been influenced. One can speculate that any change in $\Delta\rho$ with stress is probably small. This is based on the effect stress has on the average resistivity of the film. The relative change in electrical resistance, ΔR, of a longitudinally strained specimen, ΔL, is given by the standard gauge factor ratio $(\Delta R/R)/(\Delta L/L)$ as used to specify strain gauge sensitivities. In a magnetostrictive material such as nickel the gauge factor can be of magnitude approximately -20, but this large value is just the magnetoresistive anisotropic effect, itself caused by stress orientation of domains. This interaction has been discussed in Section ID(4). If the magnetoresistive effect is eliminated by magnetic saturation the gauge factor drops to about -2. It is estimated that a residual stress of 10^{10} dynes/cm^2 could cause a change in $\Delta R/R$ of 4×10^{-3}. The change in ρ_{av} would be less than 0.5%, and this would have a negligible effect on the anisotropic magnetoresistance ratio—considerably less than the experimental scatter found, for example, for permalloy in Fig. 6. Annealing of the films may reduce or increase the residual stress.

b) *Substrates* for films are an important consideration in obtaining the best magnetic properties and design parameters for a particular application. The stress effects discussed in the previous section would be enhanced if the thermal expansion mismatch of the film and substrate is large. At room tempera-

ture typical values of the thermal expansion coefficient α for commonly used substrates are about $\frac{1}{3}$ that of metals and alloys, which have values of α between 11 and 15.10^{-6}, where $\alpha = (1/L) \, dL/dT$ and the units of α are $\deg^{-1}$. For example, $\alpha \approx 3.5 \times 10^{-6}$ for Si and 4.5×10^{-6} for glass slides. It is possible to choose a substrate that matches the alloy. Mica is an example, but no work has been reported on this material.

There are two practical considerations that should be taken into account in choosing substrates. The first involves thermal conductivity. Si has one of the highest thermal conductivities (for an electrical insulator) and therefore is an ideal choice for dissipating ohmic heating. In certain cases, current densities of 10^6 A/cm^2 can be tolerated. Si is superior to Al_2O_3 except perhaps for single crystals with the c axis of the Al_2O_3 perpendicular to the plane of the film. The second practical consideration is the smoothness of the substrate. A rough surface leads to a rough film with increased surface scattering of conduction electrons and degraded magnetic properties. The increase in ρ_{av} causes a significant lowering of the ratio $\Delta\rho/\rho_{av}$. For example, unpolished BeO substrates with a roughness of 5 to 10 microinches increase the resistivity of a $Ni_{0.67}Co_{0.3}Cr_{0.03}$ 400 Å thick film as given in Table IV by a factor of two. The Al_2O_3, Si, and SiO_2 substrates show no significant difference.

c) *Inhomogeneity and imperfections* can have measurable effects on film samples. Present-day techniques of preparing films [26] [34] using high vacuum, e-gun heating and ingots with alloy compositions that take into account vapor pressures of each element give homogeneous films. However, early work on films sometimes exhibited problems involving stratification during preparation, as described by Oldfield [75]. He found that films evaporated from an alloy of composition $Ni_{81.5}Fe_{18.5}$ onto a glass substrate at 300°C had a nickel-rich interfacial layer (94Ni6Fe). The compositional gradient could extend 100 Å into the film.

The effect of dislocations on the electrical resistance and the magnetoresistance anisotropy in nickel foils has been studied by Schwerer and Silcox [76]. At room temperature dislocations make a negligible contribution to the resistivity. At low temperature (80°K) the resistivity increment $\delta\rho_D$ due to dislocations of density D per cm^2 is $\Delta\rho_D \simeq 10^{-12}D$ $\mu\Omega cm$. For annealed samples $D \simeq 10^8$ and the effect is negligible. For strained samples $D \simeq 10^{11}$ giving $\delta\rho_D \approx 0.1$ $\mu\Omega cm$. This is about the same magnitude of change in resistivity caused by residual stress in films. There is also a detrimental effect that dislocation density has on the coercive field. For example, in nickel foils at room temperature H_c increases with dislocation density according to the relation $H_c \simeq 1.4 \times 10^{-4} \sqrt{D}$ [76].

The anisotropic magnetoresistance of pure nickel at 4.2°K for high values of D and annealed samples having low D is shown in Fig. 18. In the deformed sample ($D \simeq 10^{11}$) there is a crossover where $\rho_\perp > \rho_\|$ at about 8 kOe while in the annealed sample $\rho_\perp$ is always greater than $\rho_\|$. The explanation is that the ordinary magnetoresistance effect dominates at all applied field values for the annealed samples, since the electronic mean free path is large. The deformations in the other samples scatter the conduction electrons and give rise to a weak extraordinary effect as discussed in Section IIB; in these samples the ordinary effect dominates only above 8 kOe. These data
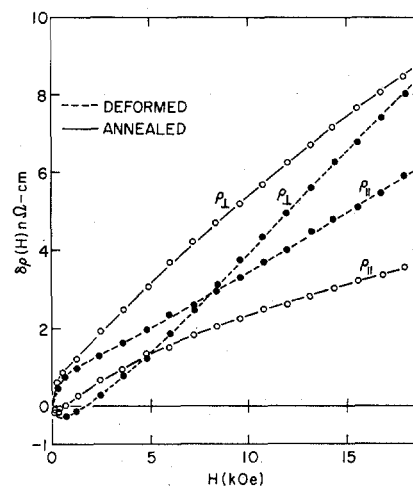

Fig. 18. Change in resistivity as a function of field for Ni foils at 4.2°K with high dislocation density and after annealing. The initial resistivity for the high dislocation density sample is

ρ (0) = 87.6 nΩcm and after annealing
ρ (0) = 32.5 nΩcm (Schwerer and Silcox [76]).

are indicative of the factors that must be considered in the interpretation of low temperature magnetoresistive measurements, especially in pure elements.

d) *Anisotropic magnetoresistance* studies of thin films are dominated by measurements on the useful alloys of permalloy composition ($\approx Ni_{0.8}Fe_{0.2}$). Ni films also have been investigated because a pure element is often considered to be more suitable for theoretical analysis. Quite recently Ni-Co films have made their appearance because Ni-Co has the largest known room temperature anisotropic ratio among the $3d$ alloys; however, it is magnetorestrictive, which gives rise to electronic noise.

In early permalloy film work by Tatsumoto et al. [77] anisotropic magnetoresistance was used to study domain motion in low frequency fields. West [78] investigated domain rotation relative to an easy axis of magnetization and showed how to determine H_k in this way. Both papers stress the advantages of using magnetoresistance to determine magnetization processes such as rotation and domain wall motion as described by Middelhoek [79]. West finds, however, that some films are inhomogeneous, with regions having deviations in the magnetic anisotropy where abrupt magnetization reversal can occur. This can be a source of Barkhausen noise.

The thickness dependence of anisotropic magnetoresistance in permalloy has been studied by several investigators [35], [80], [81]. Mitchel et al. [35] cover not only permalloy (Table IV) but a range of compositions. As previously noted for permalloy, $\Delta\rho$ is independent of thickness; it is ρ_{av} that changes. Also from this paper is taken Fig. 19, which indicates that Ni_xFe_{1-x} films (2500 Å thick) do not agree with bulk values for all values of x. The cause of this difference is attributed to magnetostriction.

The anisotropic magnetoresistance of Ni-Co films has been studied by Asama et al. [82], who find for a $Ni_{0.7}Co_{0.3}$ film of 300 Å thickness $\Delta\rho/\rho_{av} \approx 3.8\%$, a value considerably larger than reported for $Ni_{0.8}Fe_{0.2}$ of 2.6% as shown in Table IV. It will also be noted from Table IV and Fig. 17 that $\Delta\rho$ for
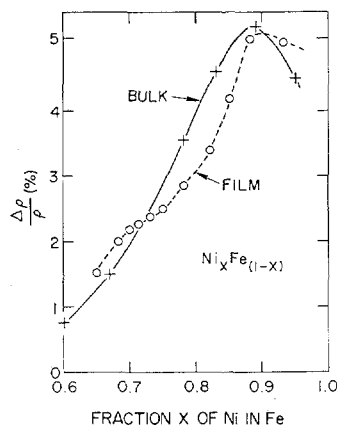
Fig. 19. Comparison of the anisotropic magnetoresistivity ratio of thin films and bulk alloys of $Ni_xFe_{(1-x)}$ as a function of composition (Mitchell *et al.* [35]).

$Ni_{0.7}Co_{0.3}$ is larger than found for $Ni_{0.8}Fe_{0.2}$. The larger value of $\Delta\rho$ coupled with a lower ρ_{av} of $Ni_{0.7}Co_{0.3}$ films are attractive features for device applications. Unfortunately $Ni_{0.7}Co_{0.3}$ exhibits large positive magnetostriction, which gives rise to Barkhausen noise problems and limits its usefulness.

Wako *et al.* [83], for pure Ni and Fe films 1000 Å thick, report $\Delta\rho/\rho_{av}$ = 1.12% and 0.17%, respectively. Ni plates down to 0.041 mm thickness have been investigated by Ehrlich and Rivier [84] to determine the effects of sample thickness at low temperatures. Normally, with films of the pure elements, conduction electrons have such long mean free paths that surface scattering dominates and it is not possible to interpret magnetoresistive effects. Ehrlich and Rivier found for their nickel, which has a large residual resistance ratio of 2200/1, evidence of surface scattering for a sample of 0.041 mm thickness. Their measurements were limited to $\Delta\rho_\perp/\rho_0$. Marsocci and Chen [85] also report on the thickness dependence on $\Delta\rho/\rho_{av}$ in nickel.

Studies of pure nickel single crystals in film form [86], [87], [88] give evidence that there is structure in the magnetoresistance with reference to the applied field magnitude and direction as discussed in Section IIA. The results are reported to be in agreement with the early work of Becker [89] and Kaya [90] on bulk single crystals. We do not attempt to compare single crystal films with polycrystalline results.

As a final comment on thin films, we mention the procedure for depositing a device film with an easy magnetic axis. This is done at an elevated temperature, about 250°C, in a magnetic field H of 50 to 100 Oe. The easy axis, which forms parallel to H, constrains the magnetic moment vector M to point in either direction along this axis in the absence of subsequent applied fields. It is the rotation of M away from the easy axis that is used in a magnetoresistive sensing device. The purpose of the easy axis, which is aligned perpendicular to the field to be sensed, is to cause magnetization of the film to proceed by rotation rather than wall motion, thus permitting high frequency operation. As far as is known, the formation of the easy axis does not affect the values of $\Delta\rho$ or ρ_{av} in a permalloy film.

EXPERIMENTAL TECHNIQUES

Bar or cylindrical samples can be measured by the standard four-probe technique, with current measured by the voltage drop across a standard resistor in series with the current probes and the same voltmeter used for the two inner probes on the sample. Potentiometers or electronic instruments can be used for the voltage measurement. The sample, of course, must be rotated in a magnetic field to get the required parallel and perpendicular orientations. The special problems associated with this four-probe measurements are discussed by Dunlap [91].

Thin films, at room temperature, can easily be measured by using a vacuum technique that forces a flexible plastic membrane in contact with the surface of the film. On the membrane are four conducting strips as shown in the schematic drawing, Fig. 20. This method can be used with either an alternating applied field or under static field conditions. Measurements can be made speedily and samples changed with ease. Temperature changes can only be made over a very limited range. It will be noted that the four-stripe technique allows a uniform current to flow across the sample and this method is identical with the four-probe point contacts along a narrow bar or wire as first mentioned.
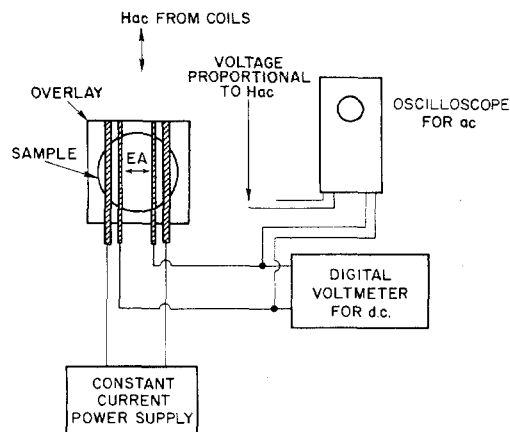

Fig. 20. Instrumentation for measuring resistivity of film samples. Arrow EA is direction of easy axis in film (Romankiw and Thompson [100]).
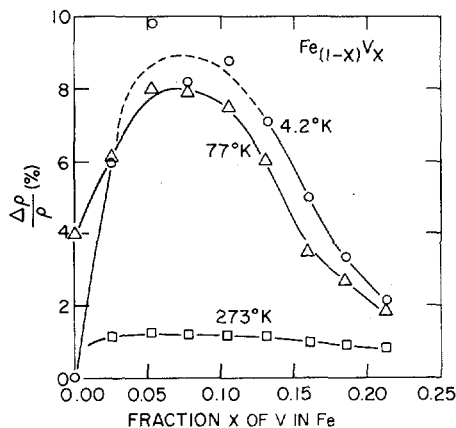

Fig. 21. A plot of the anisotropic magnetoresistivity ratio as a function of alloy composition for $Fe_{1-x}V_x$ (Sueda and Fujiwara [67]).

A technique that is simple to use and extremely flexible in obtaining all types of transport measurements is the van der Pauw method [92]. It is designed for film and foil samples of uniform thickness, but the samples do not have to be of uniform shape. Special consideration must be given to anisotropic effects as discussed by van der Pauw [93], Wasscher [94], [95], and Montgomery [96]. The pseudo Hall (also called planar Hall) measurement of anisotropic magnetoresistance has been discussed by Wu ding Ke [97].

REFERENCES

[1] W. Thomson, "On the electro-dynamic qualities of metals: Effects of magnetization on the electric conductivity of nickel and iron," Proc. Roy. Soc., vol. 8, pp. 546–550, 1857.

[2] D. A. Thompson, L. T. Romankiw, and A. F. Mayadas, "Applications of thin film magnetoresistive transducers," IEEE Trans. Mag.; vol MAG pp. 1975. (this issue).

[3] J. Smit, "Magnetoresistance of ferromagnetic metals and alloys at low temperatures," Physica, vol. XVI, No. 6, pp. 612–627, June 1951.

[4] N. F. Mott and H. H. Wills, Resistance and theremoelectric properties of the transition metals," Proc. Roy. Soc., vol. A 156, pp. 368–382, 1936.

[5] G. T. Meaden, "Conduction electron scattering and the resistance of the magnetic elements," Cont. Phys.; vol. 12, No. 4, 313–337, 1971.

[6] L. W. McKeehan, "Electrical resistance of nickel and permalloy wires as affected by longitudinal magnetization and tension," Phys. Rev., vol. 36, pp. 948–977, Sept. 1930.

[7] R. M. Bozorth, "Magnetoresistance and domain theory of iron-nickel alloys," Phys, Rev. vol. 70, pp. 923–932, Dec. 1946.

[8] Y. Shirakawa, "Magnetoresistance in Co-Ni alloys," Sci. Rept. Tohoku Univ., Honda vol. pp. 1–26, 1936.

[9] R. M. Bozorth, "Ferromagnetism" D. van Nostrand. New York 1951.

[10] H. C. van Elst, "The anisotropy in the magneto-resistance of some nickel alloys," Physica, vol. 25, pp. 708–720, 1959.

[11] J. L. Snoek, "The Weiss-Heisenberg theory of ferromagnetism and a new rule concerning magnetostriction and magnetoresistance," Nature, vol. 163, pp. 837–838, 1949.

[12] B. Luthi, "Magnetoresistance measurements of metals in high fields," Helv. Phys. Acta., vol. 29, pp. 217–219, 1956.

[13] M. Kohler "Thoery of magnetoresistance in metals," Ann. Physik, vol. 6, pp. 18–38, 1949.

[14] R. S. Allgaier, "Galvanomagnetic properties of the simplest transport model," Phys. Rev., vol. B-8, pp. 4470–4474, Nov. 1973.

[15] J. P. Jan, "Galvanomagnetic and thermomagnetic effects in metals," Solid State Physics, vol. 5, F. Seitz and D. Turnbull Eds. New York, Academic Press, 1957, pp. 1–96.

[16] S. Shtrikman and H. Thomas, "Remarks on linear magnetoresistance and magento-heat-conductivity," Solid State Commun. vol. 3, No. 7, pp. 147–150, July, 1965.

[17] Y. Gondo and Z. Funatoyawa, "On the temperature dependency of magneto-resistance of iron single crystal", J. Phys. Soc. Japan, vol. 7, No. 1, pp. 41–43, Jan–Feb., 1952.

[18] D. C. Price and G. Williams, "Two current conduction in ferromagnetic transition metal alloys." J. Phys. F: Metal Phys. vol. 3, pp. 810–824, April, 1973.

[19] T. R. McGruie and R. J. Gambino, "Magnetoresistance of pure cobalt". To be published.

[20] T. R. McGuire "Magnetoresistance anisotrophy in ferromagnetic Ni-Co alloys" AIP Conf. Proc., to be published, 1975.

[21] T. Hiraoka and M. Suzuki, "Magnetoresistance effect in single crystal of Gd," J. Phys. Soc. Japan, vol. 31, No. 5, pp. 1361–1365, Nov. 1971.

[22] R. V. Colvin, S. Legvold and F. H. Spedding, "Electrical resistivity of heavy rare-earth metals," Phys. Rev. vol. 120, No. 3, pp. 741–745, Nov. 1960.

[23] A. R. Mackintosh and L. E. Spanel, "Magnetoresistance in rare earth single crystals," Sol. State Comm. vol. 2, pp. 383–386, 1964.

[24] H. Nagasawa, "Magnetoresistance of neodymium metal", Phys. Letters, vol. 41A, pp. 39–40, Aug. 1972.

[25] S. Krongelb, A. Gangulee and G. Das, "Annealing of thin magnetic permalloy films," IEEE Trans. Mag. vol. MAG-9, pp. 568–670, 1973.

[26] K. L. Chopra, "Thin Film Phenomena," Chap. VI McGraw-Hill, New York, 1969.

[27] M. Shatzkes, P. Chaudhari, A. Levi and A. F. Mayadas, "Twin boundary resistivity" Phys. Rev. B, vol. 7 pp. 5058–5062, June 1973.

[28] E. Klokholm, "Piezoresistance in evaporated nickel films," J. Vac. Sci. Technol. vol. 10, No. 1, pp. 235–237, Jan./Feb., 1973.

[29] H. M. Rosenberg, "Low Temperature Solid State Physics," Chap. 4, Oxford Press, London, 1963.

[30] T. R. McGuire, W. D. Grobman, and D. E. Eastman, "Photoemission studies of Ni-Co alloys having large anisotropic magnetoresistance," AIP Conf. Proc. vol. 18, pp. 903–908, 1973.

[31] T. Farrell and D. Greig, "The electrical resistivity of nickel and its alloys" J. Phys. C (Proc. Phys. Soc.) Ser. 2, vol. 1, pp. 1359–1369, 1968.

[32] K. Fuchs, "Conductivity of thin metallic films," Proc. Cambridge Phil. Soc., vol. 34, pp. 100–108, 1938.

[33] E. H. Sondheimer, "The mean free path of electrons in metals," Adv. in Phys. vol. 1, pp. 1–42, 1952.

[34] R. W. Berry, P. M. Hall and M. T. Harris, "Thin Film Technology", Chap. 6 Van Nostrand Reinhold, New York, 1968.

[35] E. N. Mitchell, H. B. Haukaas, H. D. Bale and J. B. Streeper, "Compositional and thickness dependence of the ferromagnetic anisotropy in resistance of iron-nickel films," J. Appl. Phys. vol. 35, No. 9, pp. 2604–2608, 1964; also F. C. Williams and E. N. Mitchell, "A study of resistance and magnetoresistance in nickel-iron thin films," Jap. J. Appl. Phys. vol. 7, No. 7, pp. 739–742, July 1968.

[36] T. R. McGuire, G. Bate, Y. T. Chen and H. D. McCabe, "The anisotropic magnetoresistance of $Ni_{.7}Co_{.3}$ films," to be published IEEE Trans. mag. 1975.

[37] A. F. Mayadas and M. Shatzkes, "Electrical resistivity model for polycrystalline films," Phys. Rev. B, vol. 1, pp. 1382–1389, 1970.

[38] R. W. Kinne, Private Communication.

[39] J. J. Went, "Linear magnetostriction of homogeneous nickel alloys," Physica, vol. XVII, No. 2, pp. 98–116, Feb. 1951.

[40] M. Yamamoto and T. Nakamichi, "Magnetostriction constants of face-centered cubic nickel-copper and nickel-cobalt alloys." Sci. Rep. Tohoku Univ. vol. A 5 pp. 168–182, 1953.

[41] H. Ashworth, D. Sengupta, G. Schnakenberg, L. Shapiro and L. Berger. "Galvanomagnetic effects, magnetostriction, and spin-orbit interaction in Cu-Ni-Fe and other ferromagnetic nickel alloys," Phys. Rev. vol. 185, pp. 792–797, Sept. 1969.

[42] Vu Dinh Ky, "Theory of the anisotropy of resistance in ferromagnetic metals" Sov. Phys. JETP, vol. 24, No. 5 pp. 995–999, May, 1967.

[43] J. Smit, "The spontaneous Hall effect in ferromagnetics," Physica vol. 21, pp. 877–887, 1955; Physica, vol. 24, pp. 39–51, Jan. 1958.

[44] R. Karplus and J. M. Luttinger, "Hall effect in ferromagnetics", Phys, Rev. vol. 95, No. 5, pp. 1154–1160, Sept. 1954.

[45] J. Kondo, "Anomalous Hall effect and magnetoresistance of ferromagnetic metals," Prog. Theor. Phys. vol. 27, No. 4, pp. 772–792, April, 1962.

[46] F. E. Maranzana, "Contributions to the theory of the anomalous Hall effect in ferro- and antiferromagnetic materials. Phys. Rev. vol. 160, No. 2, pp. 421–429, Aug. 1967.

[47] L. Berger, "Influence of spin-orbit interaction on the transport processes in ferromagnetic nickel alloys," Physica, vol. 138, No. 4A, pp. 1083–1087, May 1965.

[48] L. Berger, "Side-jump mechanism for the Hall effect in ferromagnets," Phys. Rev. B, vol. 2, No. 11, pp. 4559–4566, Dec. 1970; Phys. Rev. B, vol. 5, pp. 1862–1869, March 1972.

[49] A. K. Majumdar and L. Berger, "Hall effect and magnetoresistance in pure Fe, Fe-Co, and Fe-Cr dilute alloys," Phys. Rev. B, vol. 7, No. 9, pp. 4203–4220, May, 1973.

[50] J. M. Luttinger, "Theory of the Hall effect in ferromagnetic substances," Phys. Rev. vol. 112, pp. 739–751, Nov. 1958.

[51] W. Kohn and J. M. Luttinger, Quantum theory of electrical transport phenomena," Phys. Rev. vol. 108, pp. 590-611, Nov. 1954.

[52] R. R. Birss, *Symmetry and Magnetism* (North-Holland Publishing Co., Amsterdam, 1964; distributed in U.S.A. by Interscience, N.Y.).

[53] Ibid, p. 70.

[54] Ibid, pp. 230-231.

[55] R. R. Birss, "The saturation magnetostriction of polycrystals", Proc. Phys. Soc. vol. 75, pp. 8-16, 1960.

[56] A. C. Smith, *et. al.*, *Electronic Conduction in Solids* (McGraw-Hill, Inc., 1967), pp. 192-202.

[57] J. W. D. Connolly, "Energy bands in ferromagnetic nickel", Phys. Rev. vol. 159, pp. 415-426, July 1967.

[58] D. H. Seib and W. E. Spicer, "Photoemission and optical studies of Cu-Ni alloys", Phys. Rev., vol. 2B, pp. 1694-1704, Sept. 1970.

[59] N. F. Mott, "The electrical conductivity of transition metals", Proc. Roy. Soc. London, vol. A 153, pp. 699-726, 1936.

[60] H. Brooks, "Ferromagnetic anisotropy and the itinerant electron model", Phys. Rev. vol. 58, pp. 909-918, Nov. 1940.

[61] L. Berger, "Influence of spin-orbit interaction on the transport processes in ferromagnetic nickel alloys, in the presence of a degeneracy of the 3d band", Physica, vol. 30, pp. 1141-1159, 1964.

[62] R. I. Potter, "Magnetoresistance anisotropy in ferromagnetic NiCu alloys", Phys. Rev. B, vol. 10, pp. 4626-4636, 1974.

[63] G. C. Fletcher, "Density of states curve for the 3d electrons in nickel," Proc. Phys. Soc. London, vol. A65, pp. 192-202, March, 1952.

[64] L. Hodges, D. R. Stone and A. V. Gold, "Field-induced changes in the band structure and Fermi surface of nickel, Phys. Rev. Letters, vol. 19, pp. 655-659, Sept. 1967.

[65] F. C. Schwerer and J. Silcox, "Low field magnetoresistance of nickel polycrystals", J. Phys. Chem. Solids, vol. 32, pp. 199-207, 1971; "Scattering effects in the magnetoresistance of nickel", Phys. Rev. B, vol. 1, No. 6, pp. 2391-2404, March 1970.

[66] J. Serre and G. Villers, "Effect Hall et magnetoresistance transverse dans Fe₇Se₈ (Structure NiAs 4c)", C. R. Acad. Sc Paris, vol. 268B, pp. 162-165, Jan. 1969.

[67] I. G. Fakidov and V. P. Krasovskiy, Magnetoresistive properties of manganese phosphides", Phys. of Metals and Metallography, vol. 7, No. 2, pp. 302-304, 1959.

[68] J. Fang, "Magnetoelectric properties of Magnetite" J. Phys. C.: Solid State Phys., vol. 7, to be published, 1975.

[69] N. Sueda and H. Fujiwara, "Magnetoresistance effects in iron-rich iron vanadium alloys", J. Sci. Hiroshima U. Ser. A, vol. 35, pp. 59-68, June 1971.

[70] T. R. McGuire, to be published.

[71] A. C. Ehrlich, J. A. Dreesen and E. M. Pugh, "Hall effect and magnetoresistance in some nickel-copper-iron alloys", Phys. Rev. vol. 133, pp. A407-A413, Jan. 1964.

[72] M. Galinier, "Some magnetic and galvanomagnetic properties of NiFeMn films", Thin Films, vol. 2, pp. 107-117, 1972.

[73] A. F. Mayadas, J. F. Janak and A. Gangulee, "Resistivity of permalloy films", JAP, vol. 45, No. 6, pp. 2780-2781, June, 1974.

[74] E. Klokholm and J. F. Freedman, "Magnetostress effects in evaporated Ni films", J. Appl. Phys., vol. 38, pp. 1354-1356, March 1967.

[75] R. C. Oldfield, "Stratification in evaporated nickel-iron films", J. Phys. D: Appl. Phys. vol. 3, pp. 1495-1496, 1970.

[76] F. C. Schwerer and J. Silcox, "Electrical resistivity due to dislocations in nickel at low temperatures", Phil. Mag. vol. 26, pp. 1105-1119, 1972.

[77] E. Tatsumoto, K. Kuwahara and M. Goto, "Magnetoresistance effect in the magnetization reversal of permalloy films", J. Phys. Soc. Japan, vol. 15, pg. 1703, 1960.

[78] F. G. West, "Magnetoresistive measurements on domain rotation in nickel-iron alloy films", Nature, vol. 188, pp. 129-130, Oct. 1960.

[79] S. Middelhoek, "Ferromagnetic domains in thin Ni-Fe films", Thesis, Drukkerij Wed. G. van Soest N. V. Amsterdam, 1961.

[80] K. Kuwahara, "Thickness dependence of the magnetoresistance effect in thin permalloy films", Trans. Jap. Inst. Metals, vol. 6, pp. 192-193, 1965.

[81] S. Krongelb, "The preparation and properties of magnetoresistive permalloy films", Jour. Electronic Mat. vol. 2, pp. 228-237, 1973.

[82] K. Asama, K. Takahashi and M. Hirano, "Ni-Co Films with large magnetoresistance for bubble detection", AIP Conf. Proc. No. 18, pp. 110-114, 1973.

[83] T. Wako, M. Saheki and T. Moreyama, "Anisotropic electrical resistance in nickel and iron films evaporated in a magnetic field", Jap. J. Appl. Phys., vol. 2, pp. 659-660, 1963.

[84] A. C. Ehrlich and D. Rivier, "Hall effect, magnetoresistance, resistivity and size effect in Ni", J. Phys. Chem. Solids vol. 29, pp. 1293-1304, 1968.

[85] T. T. Chen and V. A. Marsocci, "Transverse magnetoresistivity anisotropy measurements and the geometrical size effect in nickel thin films", J. Appl. Phys. vol. 43, pp. 1554-1558, April 1972.

[86] V. A. Marsocci, "Magnetoresistance and Hall-voltage measurements on Single-crystal Ni and Ni-Fe thin films", J. Appl. Phys. vol. 35, pp. 774-775, March 1964.

[87] V. A. Marsocci, "Effect of spin-orbit interaction on the magnetoresistance of single-crystal nickel and nickel-iron thin films", Phys. Rev. vol. 137, No. 6A pp. A 1842-A 1846, March 1965.

[88] D. C. Larson, J. E. Christopher, R. V. Coleman and A. Isin, "Magnetoresistance of nickel and iron single-crystal films. J. Vac. Sci. Tech. vol. 6, pp. 670-672, 1969.

[89] W. Doring, "Dependence of resistance of Ni crystals on direction of spontaneous magnetization", Ann. Physik, vol. 32, pp. 259-276, 1938. (Results of this paper and Kaya [90] will be found in Bozorth [9] pp. 764-766).

[90] S. Kaya, "Magneto-resistance effect in single crystal of Ni", Sci. Rept. Tohoku Univ. First Ser., vol. 17, pp. 1027-1037, 1928.

[91] W. Crawford Dunlap, Jr., "Conductivity measurements on solids", in *Methods of Experimental Physics*, Ed. by K. Lark-Horovitz and V. A. Johnson, vol. 6 B, pp. 32-71, Academic Press, New York, 1959.

[92] L. J. van der Pauw, "A method of measuring specific resistivity and Hall effect of discs of arbitrary shape", Philips Res. Repts. vol. 13, pp. 1-9, Feb. 1958.

[93] L. J. van der Pauw, "Determination of resistivity tensor and Hall tensor of anisotropic conductors", Philips Res. Repts., vol. 16, pp. 190-195, July, 1966.

[94] J. D. Wasscher, "Note on four-point resistivity measurements on anisotropic conductors", Philips Res. Repts., vol. 16, pp. 301-306, Aug. 1961.

[95] J. D. Wasscher "Electrical transport phenomena in MnTe an antiferromagnetic semiconductor" Thesis, Technische Hogeschool, Eindhoven, 30 Sept., 1969.

[96] H. C. Montgomery, "Method for measuring electrical resistivity of anisotropic materials", J. Appl. Phys. vol. 42, pp. 2971-2975, June, 1961.

[97] Wu ding Ke "Concerning the planar effect in thin ferromagnetic films", Bull. Acad. Sci. USSR, Phys. Ser. vol. 29, No. 4, pp. 581-584, April, 1965.

[98] R. M. Bozorth, T. R. McGuire, and R. R. Hudson, "Magnetic properties of materials", in *AIP Physics Handbook*, E. E. Gray Ed. 3rd ed. New York: McGraw-Hill, 1972.

[99] E. Vogt and M. Hohl, "Magnetic properties of elements and alloys" *Landolt-Bornstein Tables*, K. H. Hellwege and A. M. Hellwedge, Eds. vol. 2, part 9, section 29.1, pp. 1-1 to 1-214, Springer-Verlag, Berlin, 1962.

[100] L. T. Romankiw and D. A. Thompson, "Magnetic Properties of Plated Films". Electrochem. Soc. Symposium Vol. Ch. XXIII, R. Sard, H. Leidheiser and F. Ogburn, Eds., Princeton, N.J. 1975.